

https://dspace.org/

Investigating the effect of size, density and shape of Iron ore particles on batch jig performance

Dzaringa Kisembo, Daniel Elvis

2024-02
University of the Witwatersrand, Johannesburg
https://hdl.handle.net/10539/38872
Dzaringa Kisembo, Daniel Elvis. (2024). Investigating the effect of size, density and shape of Iron ore particles on batch jig performance. [Master's dissertation, University of the Witwatersrand, Johannesburg]. WIReDSpace. https://hdl.handle.net/10539/38872

Downloaded from a DSpace repository. https://dspace.org/



UNIVERSITY OF THE
WITWATERSRAND,
JOHANNESBURG

Investigating the effect of size, density and shape of Iron ore particles on batch jig performance

MSc (50/50) RESEARCH REPORT

Prepared by

Daniel Elvis Dzaringa Kisembo

2286841

Supervisor:

Prof. Lorenzo Woollacott

Submitted to

School of Chemical and Metallurgical Engineering

Faculty of Engineering and the Built Environment

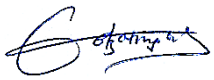
University of the Witwatersrand

Johannesburg, South Africa

October 2023

Declaration

I declare that this research report is entirely my own work, with the assistance and guidance of my supervisor. It is being submitted in partial fulfilment of the requirements for the Degree of Master of Science in Engineering at the University of the Witwatersrand in Johannesburg and has not been previously submitted for any degree or examination at any other institution.



Daniel Elvis Dzaringa

Abstract

The gravity separation method is one of the oldest methods of mineral beneficiation that takes advantage of the difference in the specific gravity of particles that are being separated. The separation occurs in a fluid medium, usually water, and involves floating off lighter material to leave behind denser ones.

There are several types of gravity separation techniques, and they vary according to the equipment that is used for the separation or the property of the medium that is being used; the main gravity separation methods that are widely used for the beneficiation of Iron ore are Jigging and Dense Medium Separation DMS.

In this research, the jigging method is selected to investigate the concentration of an Iron ore by using a batch laboratory Jig; the jigging method was preferred for its simplicity and availability, generally Jigging has several advantages, some of which include cost-effectiveness and simplicity of operation and its minimum impact on the environment.

During the beneficiation of minerals using the jigging method of ore concentration, several feed material characteristics affect the efficiency, such as the particle density, size and shape. The aim of this research was to investigate the effect of these feed properties on jig performance. Tests were conducted on a Hematite ore sample using a batch jig to gain a deeper understanding of how the density, the size and shape of particles affect segregation. The iron ore samples were screened and any extremely small particles were removed, maintaining a particle size range between 2.8 and 10 mm.

The results showed that particles were stratified on the basis of their specific gravity, denser particles reported toward the bottom layer of the bed and separated more efficiently. Less denser particles reported more toward the upper layer of the bed and were less efficiently separated. Coarser particles tend to report to the bottom layer of the bed and finer particles to the top product layer. Particles that were flatter and more elongated tended to end up in the bottom layer of the bed more often, while more rounded particles were not as likely to be found in the bottom layer.

Dedication

To my Farther, J.R. Dzaringa and my mother, E. Uronya, who have always been my guiding light, my rock, and my unwavering support. To my brothers and sisters, who have always been there for me through the good and the bad, thank you for your love and encouragement. To my friends, who have been a constant source of inspiration and laughter, thank you for being a part of my journey. This report is dedicated to all of you. Thank you for being my guiding stars.

Acknowledgements

I am extremely thankful to the Lord for providing me with the capability and opportunity to finish my master's project with success. It was only through His grace that I was able to persevere and successfully complete every aspect of this project.

I would like to express my heartfelt gratitude to my supervisor, Professor L. C. Woollacott, for his guidance, support, and encouragement throughout the course of this research. His invaluable insights and expertise have been instrumental in shaping the direction and outcome of this dissertation. It was a privilege to work with him.

I am deeply grateful to Mr. Paul den Hoed, from the School of Chemical and Metallurgical Engineering, and Mr. Sandip Naik from Anglo Research, for providing me with the necessary resources, facilities, and support to conduct this research.

Finally, I would like to acknowledge the support and encouragement of my family and friends, who have been a constant source of motivation throughout this journey.

Table of contents

Declaration ii
Abstract iii
Dedication iv
Acknowledgements v
Chapter 1: Introduction 1
1.1. Background 1
1.2. Research Objectives 2
Chapter 2: Literature Review 3
2.1. Jigging concept and separation process 3
2.2. Types of jigging equipment 4
2.2.1. Conventional Jig 4
2.2.2. In-Line Pressure Jigs 5
2.2.3. Centrifugal Jigs 5
2.3. Advantages and disadvantages of Jigging 5
2.4. Feed characteristics that affect particle stratification processes in a jig 6
2.4.1. Particle Density 6
2.4.2. Particle size 7
2.4.3. Particle shape 7
2.5. Previous studies on the beneficiation of iron ore by gravity concentration 8
Chapter 3: Methodology 9
3.1. Introduction 9
3.2. Description of equipment used 9
3.2.1. The Jig 9
3.2.2. RhoVol 11
3.3. Feed material and feed preparation 13
3.4. Experimental procedure 14
Chapter 4: Results and discussion 16
4.1. Introduction 16
4.2. RhoVol data presentation 16
4.2.1. MATLAB data output 17
4.3. Analysis of the result 19

4.3.1. Particles distributions....19
4.3.2. Partition curve....21
4.4. Influence of particle density on Jig performance....23
4.5. Influence of particle size on jig performance....25
4.6. Modelling the effect of yield and particle size on the partition curves....29
4.6.1. Summary of the effect of particle size on jig performance....32
4.7. Influence of particle shape on jig performance....32
4.7.1. Effect of shape on partition curves for particles in the size class 5 (5.86mm) at different yields....32
4.7.2. Effect of shape on partition curves for particles in size class 6 (4.9mm) at different yields....34
4.7.3. Effect of shape on partition curves for particles in size class 7 (3.94mm) at different yields....36
4.7.4. Evaluation of particle shape effect on cut density and EPM as cut height increases....38
4.7.5. Summary of the effect of shape on cut density and EPM....40
4.7.6. Effect of shape on partition numbers....40
4.7.7. Summary of findings on the effect of shape on stratification....44
Chapter 5: Discussion and conclusion....45
5.1. Discussion....45
5.2. Limitations of the study....47
5.3. Conclusion....47
References....49

List of figures

Figure 1: Photograph of the laboratory batch jig used for the experiment (i) Rear view, (ii) Front view, (iii) Rings and bed support screen, (iv) Clamped rings. 10
Figure 2: Photograph showing the full setup of the Jig chamber. 11
Figure 3: The multistage internal operations of the RhoVol device. 12
Figure 4: An example of how the RhoVol device produces a 3D model of a particle's volume. 13
Figure 5: Photograph of a Hematite subsample after screening. 14
Figure 6: An example of RhoVol results in Microsoft Excel. 17
Figure 7: Number of particles in 8×8 density and size classes. 18
Figure 8: Number of particles in 12×12 density and size classes. 19
Figure 9: Density distribution graph. 19
Figure 10: Size distribution graph. 20
Figure 11: Shape distribution graph. 20
Figure 12: Density-Size 3D distribution. 21
Figure 13: Empirical equations for density separations in mineral processing units (King, 2001). 23
Figure 14: Density partition curve graph. 24
Figure 15: Density partition curves for different particle sizes for different yields. ...26
Figure 16: Graph showing the effect of particle size on density partition number of particles with SG=4.231 27
Figure 17: Effect of size on EPM & cut density at different %yield. 28
Figure 18: Effect of Yield on the linear fits of Cut density vs Particle size. 29
Figure 19: Example of fits of the overall linear model to the partition data. Crosses indicate partition numbers for all data points. Ringed crosses indicate which are 'reliable' because they are derived from classes with more than 50 particles. 31
Figure 20: Effect of shape on partition curves for particles in size class 5 with 16% and 39% Yields (i.e., cutting the bed at the top of layers 1 and 2). 33
Figure 21: Effect of shape on partition curves in size class 5 (5.86mm) with 54%, 69% and 83% Yields (i.e., cutting the bed at the top of layers 3, 4 and 5). 34

Figure 22: Effect of shape on density partition curves for size class 6 (4.9mm) particles for different yields.....35
Figure 23: Effect of shape on density partition curves in size class 7 (3.94mm) for different yields.....37
Figure 24: Effect of shape on EPM and cut density in size class 5 at different yields. 38
Figure 25: Effect of shape on EPM and cut density in size class 6 at different yields. 39
Figure 26: Effect of shape on EPM and cut density in size class 7 at different yields. 39
Figure 27: Effect of shape on size class 5 (5.86mm) and (i) SG class 1; (ii)SG class 2; (iii) SG class3; (iv) SG class 4 at different yields. 41
Figure 28: Effect of shape on size class 6 (4.96mm) and (i) SG class 1; (ii)SG class 2; (iii) SG class3; (iv) SG class 4 at different yields. 42
Figure 29: Effect of shape on size class 7 (3.94mm) and (i) SG class 1; (ii)SG class 2; (iii) SG class3; (iv) SG class 4 at different yields. 43
Figure 30: Effect of size on EPM and cut density at 16% yield.....51
Figure 31: Effect of size on EPM and cut density at 39% yield.....52
Figure 32: Effect of size on EPM and cut density at 54% yield.....53
Figure 33:Effect of size on EPM and cut density at 69% yield.....54
Figure 34: Effect of size on EPM and cut density at 83% yield.....55
Figure 35: Partition Curves for different sizes. 55

List of tables

Table 1: Advantages and disadvantages of Jigging. 5
Table 2: Test duration for each test run 14
Table 3: Percentage yield for cutting the bed at the top of each layer.....24
Table 4: Linear fit parameters for Cut Density vs Particle size. 28
Table 5: Linear fit parameters for EPM vs Particle size. 29
Table 6: Table showing the influence of size on EPM and cut density at 16% yield...51
Table 7: Table showing the influence of size on EPM and cut density at 39% yield...51
Table 8: Table showing the influence of size on EPM and cut density at 54% yield...52
Table 9: Table showing the influence of size on EPM and cut density at 69% yield...53

Table 10: Table showing the influence of size on EPM and cut density at 83% yield.54
Table 11: Fit LOG data.....56
Table 12: Partition data for SG class 3. 56
Table 13: Parameters for linear fits to plot.....56
Table 14: MATLAB output data for 8x8x4 classes. 57

Chapter 1: Introduction

1.1. Background

Mineral concentration is the process of separating valuable minerals from waste minerals using physical techniques. Different methods are used in the metallurgical industry, such as gravity separation, which is based on the density difference between the valuable mineral and the waste mineral. A common gravity separation technique is jigging, which uses fluid movement to separate particles of different densities in a bed, and then removing the different layers.

Mineral jigging is a widely used technique for the beneficiation of iron ore due to its several advantages. One of the main benefits is its cost-effectiveness, it has a lower operating cost per unit of output compared to other methods. Additionally, it is relatively simple to operate, making it a user-friendly option. Another advantage of mineral jigging is its minimal environmental impact as it does not require the use of chemicals, making it a more sustainable option. Furthermore, jigging is a well-established method that has been widely used in the mineral processing industry for many years, and it has proved to be an effective method for the concentration of iron ore (Burt, 1999).

Mineral jigging is a long-established method of mineral beneficiation, but the underlying principles of particle stratification to enable separate removal in jigs are not yet fully understood. Despite this, recent advancements in research have led to the development of models to better understand the dynamics of particle segregation in jig systems, such as the work by Mehrotra and Mishra (1997) which used a numerical model called Discrete Element Method (DEM) to simulate particle stratification in jigs. Karantzavelos and Frangiscos (1984) have attempted to identify the operating variables that affect particle stratification in jigs through the use of empirical models. These variables have been divided into two groups: disturbance variables and manipulated variables. Disturbance variables are characteristics of the minerals in the feed, such as particle shape, size, density, etc. while manipulated variables refer to the conditions under which the jigging process is operated. For the simplicity of the investigation, only the disturbance variables will be considered. However, even when

the focus is on disturbance variables, not all the feed characteristics are accounted for in the jig models that have been developed; many researchers focused only on the effect of variations in mineral density while assuming that the feed is mono-sized and uniformly shaped (Mayer.F., 1964); (Tavares, L.M. & King, R.P., 1995).

Few studies have been conducted to understand the effect of variations in both particle size and mineral density on stratification in jigs, with only a handful of researchers such as Tavares (1999) and Rao (2007) having attempted to conduct simulation studies on the topic. Additionally, there is limited research available on the effect of particle shape on stratification in jigs.

The study presented in this report will attempt to understand the role played by three disturbance variables, namely mineral density, particle size and shape during the separation by jigging. Therefore, the effect of other operating parameters will not be considered for this project.

1.2. Research Objectives

The primary aim of this study is to investigate the influence of size, density and shape of iron ore particles on the separation efficiency in a Jig.

The following questions will be addressed to meet our research objectives:

- How does the particle's density affect jig performance?
- How does particle size affect jig performance?
- How does particle shape affect jig performance?
- What are the practical implications of the findings?

Chapter 2: Literature Review

2.1. Jigging concept and separation process

Gravity concentration methods aim to create conditions that allow particles of varying density, size, and shape to move relative to one another due to gravity or centrifugal forces acting upon them and creating different layers containing light and denser materials and fine and coarser particles. In Jigging, the interparticle movement is caused by the particle bed's vertical expansion and contraction due to fluid pulses (Mukherjee, A.K. & Mishra, B.K., 2006). Although the system has experienced significant development over the past years, the basic principle of stratification has remained the same in different operations and equipment, whether in a conventional continuous jig or a batch jig. The separation of particles takes advantage of the difference in specific gravity of materials that undergo a pulsating vertical movement in a fluidised bed due to the fluid injected from the bottom of the bed at a given pulsating rate. Jinnouchi *et al.* (1984) studied the mechanism of pulsating water, how the amplitude and frequency of pulsation regulate water velocity and its influence on particle separation. However, the dynamics of bed expansion and its relation to particle separation were not explained.

In a jigging process, the feed is introduced into a jig chamber filled with water and forms a bed of particles beneath the surface. The particle bed sits on top of a jig support screen through which water is being pulsed vertically from below to enter the jig chamber. The upward stroke or pulsation and a downward stroke or suction, which characterise the jigging action, are subdivided into the inlet, expansion, exhaust, and compression stages, forming the four phases of a jigging cycle (Mehrotra, S.P. & Mishra, B.K., 1997). At the inlet stage, the bed of particles is lifted by the upward stroke of the jigging mechanism. The expansion stage takes place near the end of the upward stroke and there is a differential upward trajectory between the lighter and denser particles, as the lighter particles continue moving upward while heavier particles decelerate. Then exhaust and compression happen during the suction or downward stroke; particles re-settle at a differential downward motion related to their density, size and shape as the bed reconsolidates to its initial volume. The repetition of the upward and downward action creates a bed stratification in which fine and low-

density particles move to the top of the bed; in contrast, coarse and high-density particles settle at the bottom of the bed. Particles with intermediate density, size and shape are located between the bed's top and bottom (Burt, 1999).

The extraction of valuable minerals becomes more straightforward after stratification. In the case of iron ore processing, the product mineral will be concentrated at the bottom just below the lighter material or waste; thus, the bottom layer will be removed and separated from the waste. However, this is not always the case in mineral beneficiation of other minerals like Coal, where the product mineral will be concentrated at the upper layer and the waste at the bottom layers (Wills, B.A. & Finch, J.A., 2016).

2.2. Types of jigging equipment

Factors that affect the design of different Jigs include the pulsating mechanism, which may be generated pneumatically, for example, in the Baum and Batac Jig or mechanically, like in the Harz and Denver Jig (Wills, B.A. & Finch, J.A., 2016).

Falconer (2003) reviewed the different types of jigs by presenting some old types and new development, where the Conventional Jig is the most ancient and in-line pressure, and centrifugal jigs are more recent types.

2.2.1. Conventional Jig

The Russell jig is a well-known type of conventional jig containing two adjacent feed compartments, each funnelling material to two sets of cells in succession. As the material streams over the two boxes, a jigging action is done to separate heavier or larger particles as an underflow concentrate after they move through the ragging on the lower part of the jig bed. The remaining material is discharged as tailings over the tailings gate into an overflow launder. One advantage of conventional jigs is their ability to recover coarse particles, which reduces the need for grinding hard rock ores and minimises the overproduction of slimes. However, conventional jigs also have some disadvantages, which include:

- Ragging screens need regular cleaning to avoid blinding and the accumulation of coarse heavy materials,

- Conventional jigs are not appropriate for the recovery of fine particles
- Water consumption is high (Falconer, 2003).

2.2.2. In-Line Pressure Jigs

In-line Pressure jigs are a fairly new invention and they function similarly to conventional jigs, except that they operate at higher pressures than atmospheric pressure. The benefits of these jigs are unparalleled, as they require minimal infrastructure to integrate into an existing production line and occupy a relatively small area in comparison to their counterparts. The disadvantages of in-line pressure jigs are similar to conventional jigs for water consumption, regular cleaning of the ragging screen, and recovery of fine particles (Falconer, 2003).

2.2.3. Centrifugal Jigs

The most well-known centrifugal Jig is the Kelsey Jig, which uses the same pulsation and ragging principle as conventional jigs. The main difference is that the Kelsey Jig achieves jigging through rotation, which creates centrifugal force, causing differential acceleration to increase and hence improving separation efficiency. The Kelsey jig was developed by taking advantage of the centrifugal force to enhance separation, especially when working with fine particles or mineral particles with a small difference in density.

Disadvantages of Centrifugal jigs are:

- Complex mechanical systems that need a daily inspection, lubrication, and regular service
- To avoid blinding, feed must be screened to a smaller size than the internal screen of the jig.
- Daily cleaning of the inner screen

Relative high capital and operating costs (Richards & Jones, T., 2004).

2.3. Advantages and disadvantages of Jigging

The table below summarises some pros and cons of using Jigging to concentrate minerals.

Table 1: Advantages and disadvantages of Jigging (Maré *et al.*, 2015).

Advantages	Disadvantages
Improves the grade of concentrate from a low-grade feed material	Reduced water clarity, affecting the performance.
Works well with both coarse and fine materials	The separation efficiency of an ordinary Jig is lower than dense medium separation.
Use of a cheap separation medium fluid (Water or air only)	It uses a large quantity of water. Hence, an efficient dewatering plant is required.
Less wear effect on connected pumps and piping system	Higher power consumption compared to an equivalent DMS circuit.
Easy maintenance	Conventional Jig is not efficient for ultrafine particles.
Centrifugal force can produce better separations.	Inefficient at wide size ranges.

2.4. Feed characteristics that affect particle stratification processes in a jig

Particle properties that play a role in stratification are the following.

2.4.1. Particle Density

Jigging's primary goal is density separation, which depends on density differences between light and dense materials. As stated previously, the stratified bed is characterised in such a way that low-density particles are predominantly found in the upper layer of the bed and high-density particles toward the bottom layer. Particles with intermediate characteristics are located between the bed's top and bottom layers. In terms of particle density, Jig separation performance is heavily influenced by near-gravity material or NGM, defined as the fraction of material whose separation density falls within 0.1 g/cm^3 of the cut density. When the feed particles contain large amounts of near-gravity material, misplacements between light and dense particles

are more likely to occur in the product (Ambrós, 2020). Effective mineral separation requires a considerable difference between the densities of valuable minerals and

gangues. Jig separation becomes more effective with increasing absolute values of the concentration criterion (cc) expressed as: $cc = \frac{\rho_h - \rho_f}{\rho_l - \rho_f}$ … (1)

Where ρ_h, ρ_f and ρ_l are respectively the density of the heavy mineral, the density of the light mineral and the density of the fluid medium (Wills, B.A. & Finch, J.A., 2016).

2.4.2. Particle size

Particle size also affects the performance of jigs during particle separation. In the literature, particle size has been extensively discussed concerning density stratification. The overall observation is that separation is less accurate the finer the feed size and more efficient as particle size in the feed increases. This is why Jigs are ideal for the concentration of minerals that can be liberated at a coarser size.

Furthermore, due to its non-monotonic nature, size segregation is more complex than density segregation. Because it involves intricate geometrical interactions between particles, different stratification patterns may result from changes in the size ratios of coarser and finer particles (Ambrós, 2020). These concerns were addressed by Woollacott and Silwamba (2016) by investigating the effects of different size ratios on size stratification in batch jigs; four different stratification patterns were observed, which suggests the complexity involved when combined density segregation is taken into account.

2.4.3. Particle shape

Another factor that can impact particle separation in a jig is variations in particle shape. Brozek and Surowiak (2007) studied the effect of particle shape on jig separation efficiency and settling velocity. They found that particles of irregular shape had a negative impact on both settling velocity and separation efficiency when compared to spherical particles.

Pita and Castilho (2016) studied the separation of plastics in a Denver jig to examine the effect of lamellar particle separation. They observed that the effect of particle shape on separation precision depended on the separating context. When separating lighter components, an increase in the proportion of lamellar particles increased separation

precision. Conversely, an increase of lamellar particles in contexts involving high-density components reduced the efficiency.

2.5. Previous studies on the beneficiation of iron ore by gravity concentration

Bosman (2007) compared Jigging and Dense Medium Separation to determine the best option for iron ore beneficiation. Based on the advantages and disadvantages of one method over the other, the study concluded that the choice between Jigging and dense medium separation is not clear-cut. Therefore, the feed characteristics and concentration costs must be considered when determining the best method for iron ore beneficiation.

Naudé *et al.* (2013) analysed iron ore separation in a prototype batch jig separator called the Mineral Density Separator (MDS). The MDS is a device for separating ore samples into various bulk-density sections and can be used to evaluate the efficiency of jigging plants. The MDS operates with the same principle as the conventional Jig; the only difference is that the MDS is a laboratory apparatus. This study involved particles painted in different colours according to their respective densities and observing how these stratified in the device.

Chapter 3: Methodology

3.1. Introduction

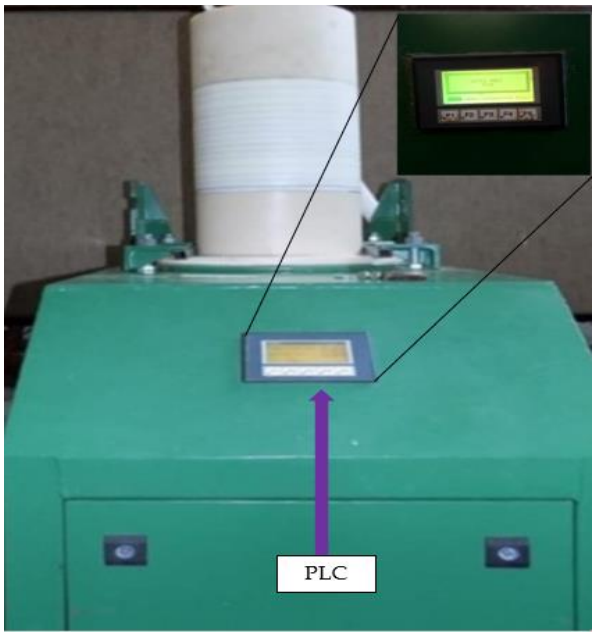
This chapter describes the methodology applied to answer the research questions, the experimental procedure, the equipment and the jigging conditions used in the project.

3.2. Description of equipment used

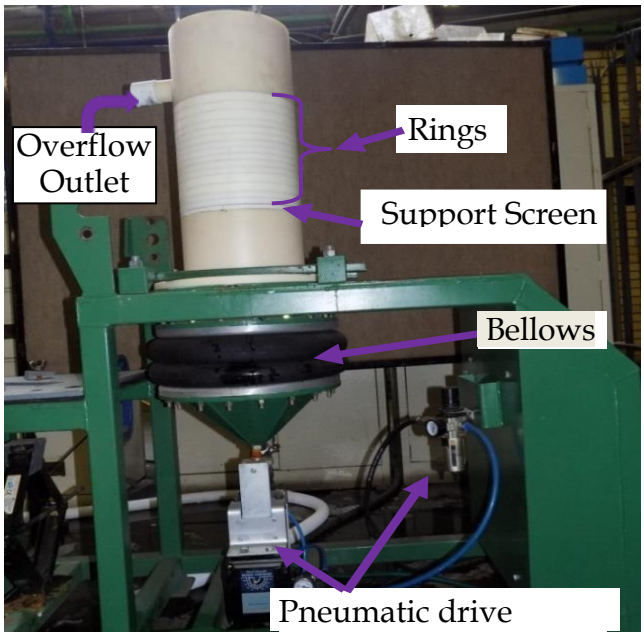
The experimental tests were carried out using a laboratory batch jig in the Mineral Processing laboratory in the School of Chemical and Metallurgical Engineering at the University of the Witwatersrand. It had a similar design to the Mineral Density Separator located at Mintek, which had been used by previous researchers such as Naudé *et al.* (2013) in their study of Iron ore jigging.

3.2.1. The Jig

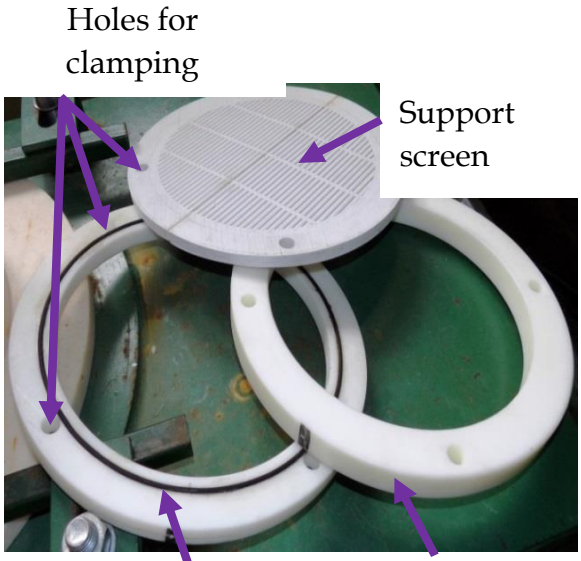
This batch jig used as illustrated in the figure 1 was composed of annular rings, 15 mm and 20mm in height, tightly clamped together to prevent leakage and formed a cylindrical chamber of 200 mm internal diameter on top of a support screen. Rings enabled the jig bed to be split into horizontal sections after jigging. A pneumatically driven bellows system located under the support screen caused pulsion and suction of the jig bed. Jigging frequency, stroke amplitude and time were adjusted using a Programmable Logic Controller (PLC).



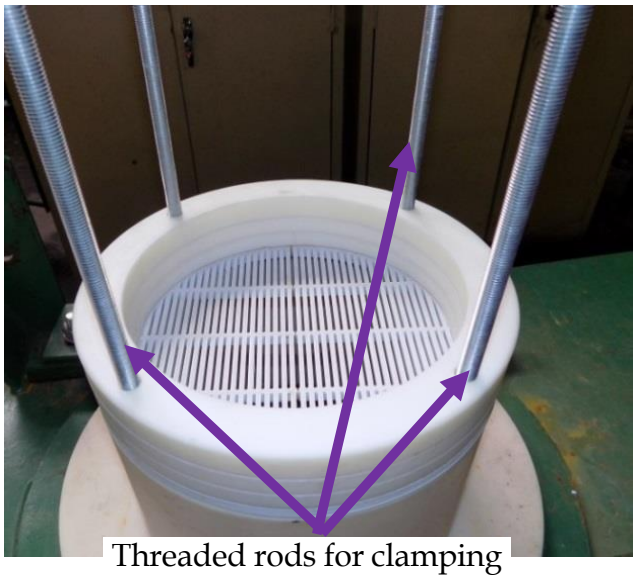
(i)



(ii)



(iii)



(iv)

Figure 1: Photograph of the laboratory batch jig used for the experiment (i) Rear view, (ii) Front view, (iii) Rings and bed support screen, (iv) Clamped rings.



Figure 2: Photograph showing the full setup of the Jig chamber.

3.2.2. RhoVol

The samples cut from the laboratory jig were dried and then processed by the RhoVol devices at the De Beers Group technology laboratory and Anglo Research Laboratory. The densities of the samples cut from the jig were measured at the Anglo Research Laboratory as well.

Fofana and Steyn (2018) reported that the RhoVol machine was developed by DebTech based on 3D silhouette models by Forbes et al. (2003). The machine uses a quick weight measurement tool to measure the mass of every particle in the sample. The size, volume, density and shape of every particle are determined from silhouette images of each particle taken as it falls through a light chamber. A 3D representation is created for each particle, making it possible to calculate various physical characteristics like particle size and shape factor (elongation, flatness, and compactness). The Rhovol can also sort the sample into discrete sorting bins depending on any of the measured particle properties to allow for further analyses of the material. Approximately 1000 particles per hour can be processed, which has been shown to be a statistically viable sample size for most materials. The multistage internal operations of the RhoVol device are shown in Figure 3; It is made up of two feeder system. The weighing mechanism incorporates high-speed load cells to

guarantee precise particle mass analysis Multiple images from several cameras, offset at different angles, are analysed simultaneously to produce the 3D volumetric model of the particle. At the same time, a particle sorting algorithm classifies particles based on their characteristics, such as density, mass, size, or shape.

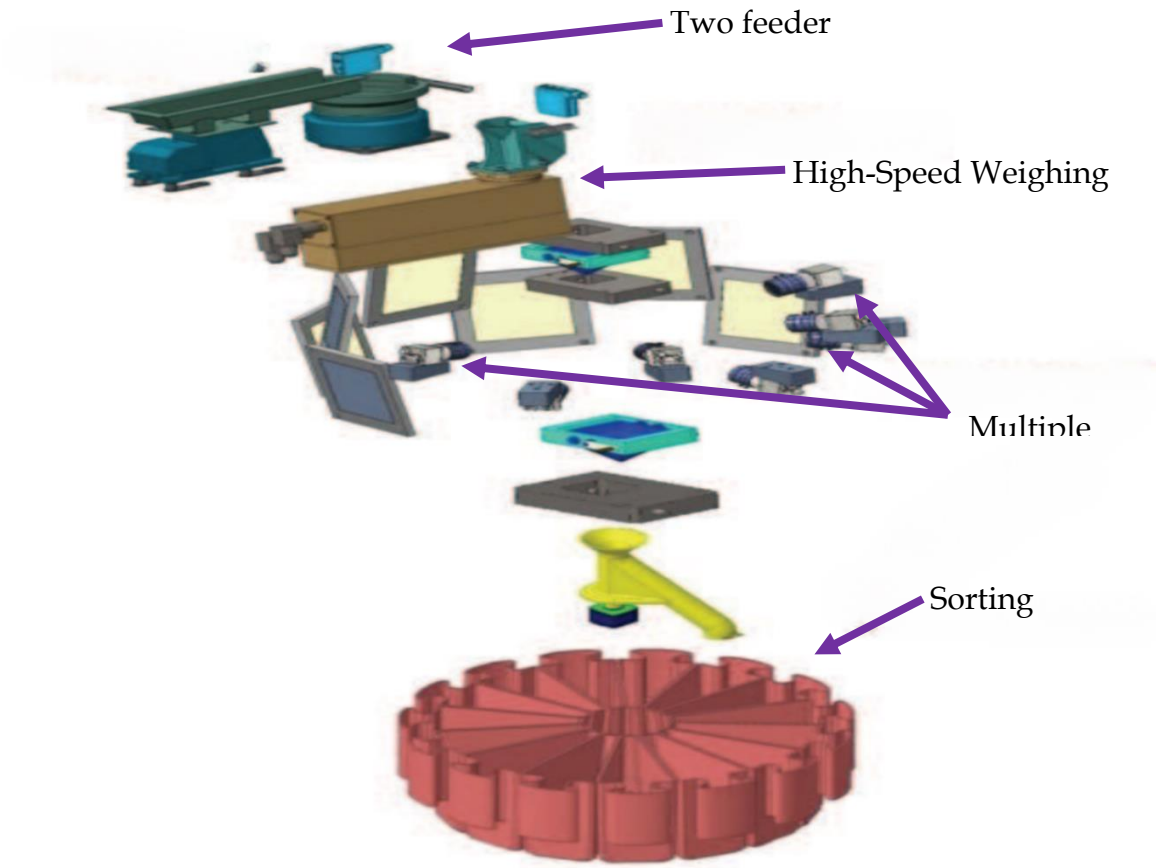


Figure 3: The multistage internal operations of the RhoVol device.

Debtech found that the most reliable measure of particle shape was the 'compactness factor'. This is calculated from the three orthogonal dimensions of a particle measured along each direction of the particle, where: "a" represents the longest dimension, "b" represents the intermediate, and "c" represents the shortest dimension. It is defined as a number less than or equal to one that represents the particle's compactness.

It is defined as $\left(\frac{bc}{a^2}\right)^{1/3}$ … (2)

According to this formula, the compactness of a sphere is unity.

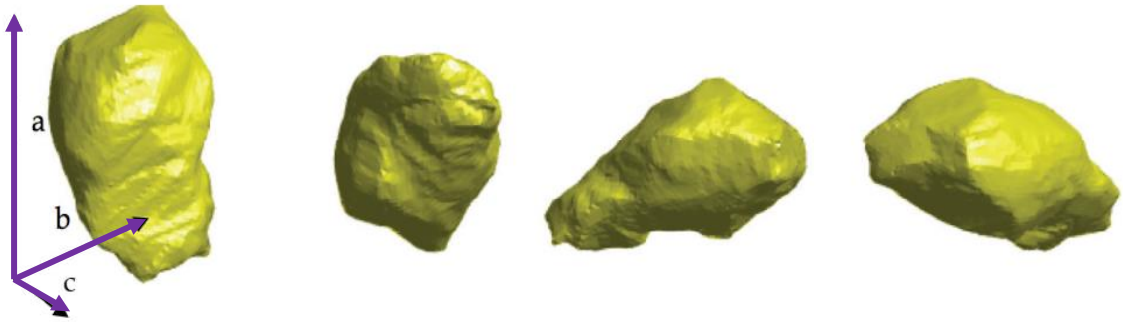


Figure 4: An example of how the RhoVol device produces a 3D model of a particle's volume.

3.3. Feed material and feed preparation

To investigate the effects of iron ore particle size, density and shape on batch jig performance, a sample of Hematite weighing about 50kg with a top particle size of 8mm was provided by Kumba Iron ore and was divided into identical subsamples of around 5kg each using a riffler to ensure consistency in sample properties. The subsamples were screened before jigging to meet the separation requirement. Only coarser particles were retained (+4mm and -8mm) for the tests, and undersize particles were discarded at this stage. Unfortunately, the sample made available for this study was a Hematite concentrate rather than feed material implying a narrow density distribution. This was discovered only after De Beers had processed the samples. The figure below shows the subsample after screening.



Figure 5: Photograph of a Hematite subsample after screening.

3.4. Experimental procedure

Four tests were carried out at different jigging times; for the first test, the jigging time was much longer to allow the system to reach an equilibrium state. Hence the first test is referred to as the equilibrium test. Below is a table summarising the duration of each test.

Table 2: Test duration for each test run

Test number	Jigging time (Seconds)
Test 1	960
Test 2	60
Test 3	300
Test 4	150

During each test, the jig chamber was set up as detailed in section 3.1.1, and a carefully mixed subsample of the feed material chosen for the test was added to the jig chamber. The chamber was then flooded with water. As a result, each test was conducted on a bed approximately the same height (roughly 130 mm). After the completion each test, the jig chamber was unclamped. A slicing tool was inserted between each ring to divide the bed into horizontal sections and each layer was cautiously removed one by

one from the top of the bed for a total of 6 layers for each test. Afterwards, the collected material from each layer was dried, bagged, labelled and analysed using the RhoVol machine. Because of the processing and analysis complexity of the results, only sample from the equilibrium test (Test 1) has been processed in this study. The other samples are the subject of a follow-up project.

Chapter 4: Results and discussion

4.1. Introduction

Experimental results and discussions are presented in this chapter, divided into three parts. The first part provides general information about the presentation of the results. It includes output from RhoVol analysis presented as an excel spreadsheet before being processed with the MATLAB analysis program. The second part presents MATLAB output data, and the model used to analyse the large amount of data obtained from RhoVol measurements. In the last part of this chapter, results are presented in the form of partition curves and are discussed to address the research questions.

4.2. RhoVol data presentation

Data captured by the RhoVol machine was recorded and presented on a Microsoft Excel spreadsheet. Figure 6 is an example of the result produced by the RhoVol machine after analysing a jig test sample. Only 6 particles are shown in this example out of 4179 particles captured by the machine for Test 2 and layer 1. The results for all 6 layers in a test (about 24000 particles) were compiled as the input file for the MATLAB analysis program. (The output is too large for inclusion in an appendix but can be made available if requested.)

RhoVol data presented anomalous measurements because of inherent errors in estimating particle volumes from silhouette images. These errors were minimised by applying a volume correction factor. (This was obtained by comparing the volume predictions from the RhoVol measurements with the equivalent volumes obtained from densities measured with a pycnometer.) However, some discrepancies remained after this correction: particles with measured densities less than 2.6 g/cc and greater than 5 g/cc. These anomalies amounted to only 1.16% of the total mass of the sample and were discarded.

RhoVol Report												
Machine I	3DT00X											
Site Name	De Beers Technologies											
Sample Na	WITS 1											
Mine Nam	-											
Operator	z											
Start Date	########											
Start Time	12:58:57											
Number o	1											
Sorting Op	Disable	Upper		Lower								
Sorting Limits		N/A		N/A								
Fed Partic	4982											
Captured	4179											
Failed Par	42											
Process Ti	05:32:52											
Mass (g)	1171.17											
Mass	Volume	Density	Minimum	Minimum	Roller Gap	Compactn	Elongation	Flatness	Number o	Bin	Transparency	
137.909	30.945	4.457	4.44	4.025	2.926	0.75	1.218	1.596	21	13	NaN	
166.397	39.266	4.238	4.87	4.165	2.775	0.682	1.451	1.497	21	13	29	
207.369	46.314	4.477	5.261	4.087	2.5	0.579	1.466	2.393	21	13	29	
73.126	26.255	2.785	4.613	3.65	1.937	0.653	1.183	2.567	21	13	31	
224.558	50.054	4.486	5.098	4.327	3.079	0.655	1.441	1.709	21	13	NaN	
395.85	92.561	4.277	5.791	5.031	4.81	0.713	1.566	1.124	21	13	26	

Figure 6: An example of RhoVol results in Microsoft Excel.

4.2.1. MATLAB data output

The data obtained from RhoVol was processed by MATLAB using a program code developed by Professor Woollacott to analyse the results and address the research questions. The program 'sorted' different particles into particle classes based on their density, size and shape factor. First, the maximum and minimum densities, sizes and shape factors were determined from the RhoVol data. Class boundaries were then calculated by dividing the density, size and shape factor ranges equally to give a pre-selected number of density, size and shape factor classes. A compromise on the number of classes had to be decided to proceed with analysing the RhoVol data. Too many classes resulted in some classes being empty or having very few particles to be considered when calculating partition numbers. Having very few numbers of classes caused a significant variation of particle properties within a class. Hence, a class's

average density, size and shape factor were not very representative of the particles in a class. Inspection of the number of particles in classes for different numbers of classes suggested between 8 and 12 density and size classes would be appropriate and between 4 and 6 shape factor classes.

Figures 7 and 8 show tables of the number of particles in each density and size class for 8×8 and 12×12 classes in the test sample. The size range for 8x8 is 0.96mm and 12x12 is 0.64mm. Density and size classes in yellow indicate those with more than 50 particles, which is the minimum number of particles a class should have to be considered when plotting the partition curve. In other words, these are the meaningful classes. The orange classes indicate classes in which the number of particles is close to the minimum number of particles a class should have to be considered when plotting partition curves, they may be useful for further analysis. The grey classes are the classes containing very few particles that are not taken into account for partition curve analysis. By comparing figure 7 and 8, it can be seen that the 12x12 classes have more grey classes and that most meaningful classes are concentrated between SG class 2 and SG class 8. On that basis, 8x8 was found to be more representative of the data, therefore, all the subsequent analysis was conducted using 8x8 classes.

8x8		density range=	0.30						
	SG class→	1	2	3	4	5	6	7	8
size class↓		4.82	4.53	4.23	3.93	3.64	3.34	3.04	2.75
1	9.69	2	11	9	6	2	0	0	0
2	8.73	13	49	46	12	6	4	1	4
3	7.78	48	186	173	63	20	7	5	11
4	6.82	142	625	501	166	61	38	26	14
5	5.86	219	1370	1072	398	133	72	46	49
6	4.90	313	2534	2224	856	345	142	70	82
7	3.94	371	3915	3903	1576	595	272	152	206
8	2.99	20	118	90	63	25	7	2	7
size range=	0.96							Total number =	23498

Figure 7: Number of particles in 8×8 density and size classes.

12x12	density range=	0.20											
	SG class→	1	2	3	4	5	6	7	8	9	10	11	12
size class↓		4.87	4.68	4.48	4.28	4.08	3.89	3.69	3.49	3.29	3.09	2.90	2.70
1	9.85	0	1	4	3	7	2	2	0	0	0	0	0
2	9.21	2	11	10	9	2	2	0	0	3	0	0	1
3	8.57	0	18	29	29	16	3	5	1	1	0	2	2
4	7.936083	5	46	77	70	28	23	10	5	1	2	1	6
5	7.297250	16	89	178	152	78	33	22	7	7	3	8	5
6	6.658417	20	198	372	301	147	71	30	27	17	17	9	5
7	6.02	22	309	603	491	260	124	58	41	25	9	21	20
8	5.38	44	484	929	786	385	201	98	65	40	38	25	23
9	4.74	36	604	1405	1241	705	357	194	112	59	35	34	42
10	4.10	44	817	2059	1964	1144	582	302	170	99	68	76	90
11	3.46	17	384	1089	1000	608	317	161	93	67	39	36	56
12	2.83	1	4	9	7	6	4	3	2	2	0	1	1
size range=	0.64										Total number =		23498

Figure 8: Number of particles in 12×12 density and size classes.

4.3. Analysis of the result

4.3.1. Particles distributions

Particle distribution graphs of density, size and shape were analysed to understand how particles were distributed in the test sample. Figure 9 shows the density distribution graph. It can be seen that more than 80% of the sample has an SG > 4.2 with only 11% having SG <4.1 and 4% less than 3.9. This indicates that the sample had already been processed and is a concentrate. One consequence of this is that sharp separations when jigging this sample are not to be expected; higher than usual EPM values are therefore to be expected.

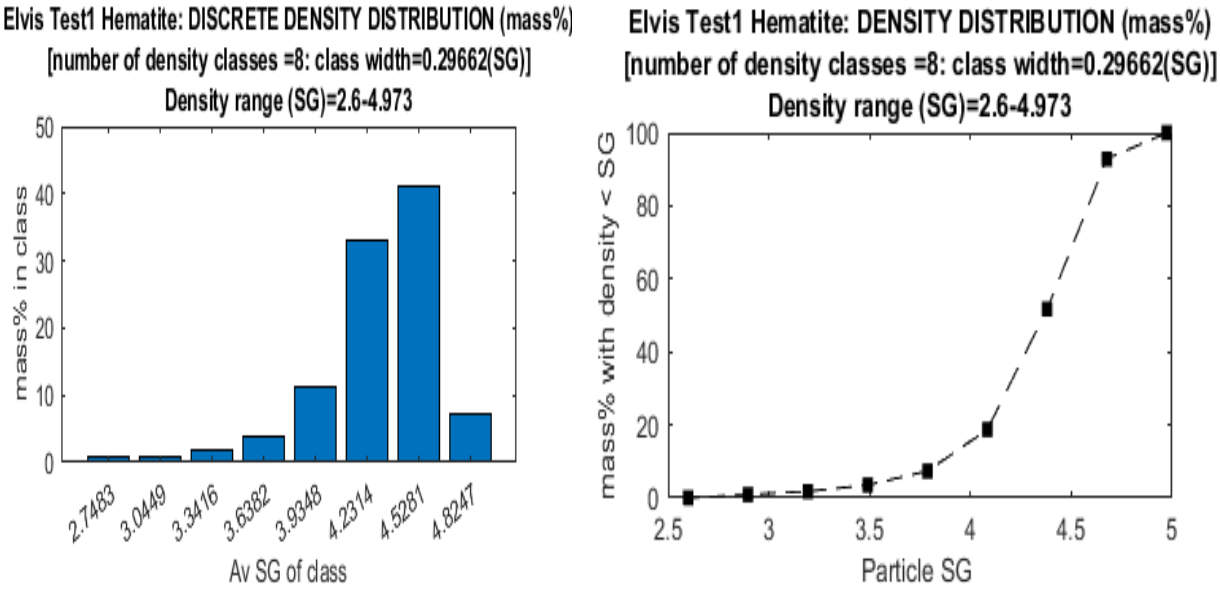


Figure 9: Density distribution graph.

Figure 10 shows the size distribution graph. It can be observed that the particle size ranges between 2.51mm and 10.17mm and 75% of the sample consisted of particles of size greater than 4.9mm. This indicates a coarse sample.

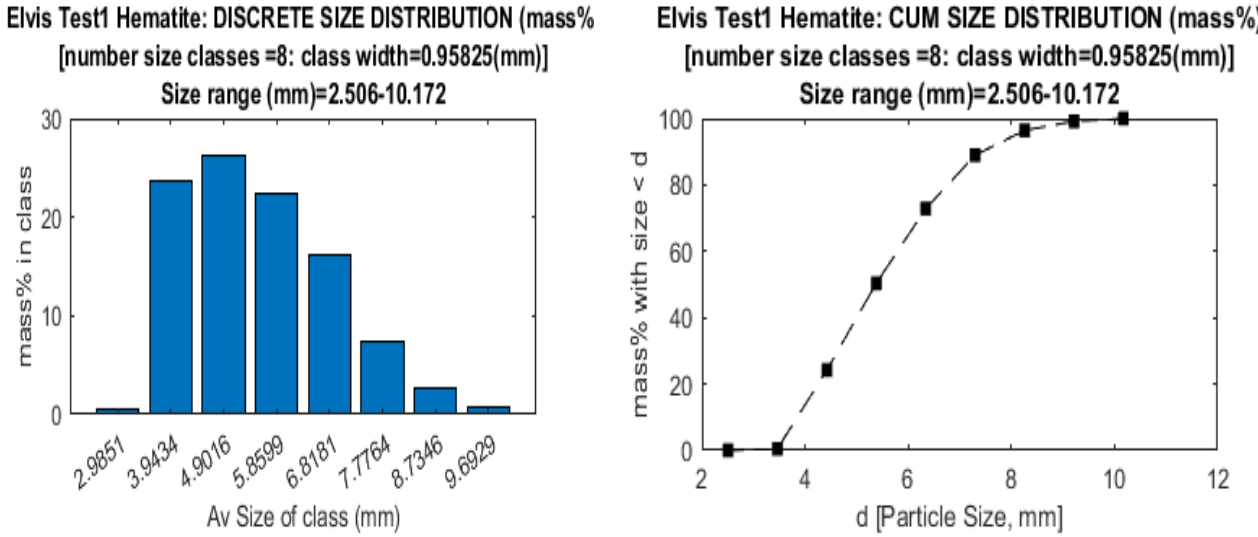


Figure 10: Size distribution graph.

Figure 11 shows shape distribution graph. It can be seen that over 60% of the sample consisted of particles with a shape factor > 0.7, and less than 2% had a shape factor <=0.44. This indicates that the sample contained very few particles flat in shape.

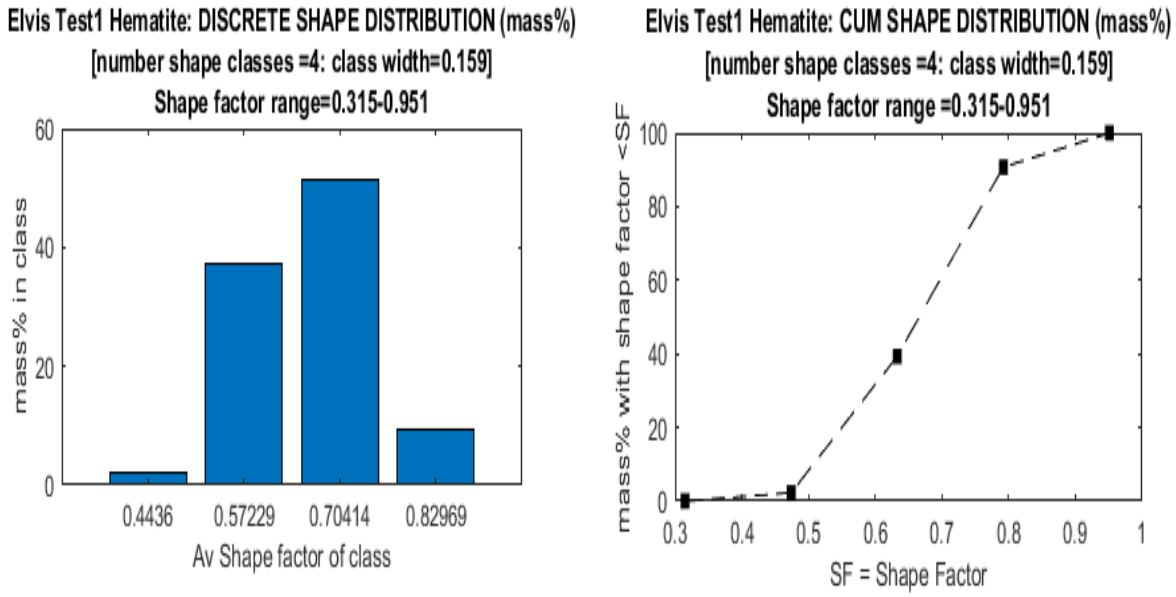


Figure 11: Shape distribution graph.

Figure 12 shows a 3D distribution of density and particle size. It can be seen that most particles in the sample are concentrated between the SG class of 3.5 and 4.5g/cc and the size class of 4 and 8mm. The distribution graphs show that the sample was a Hematite concentrate with coarse particles.

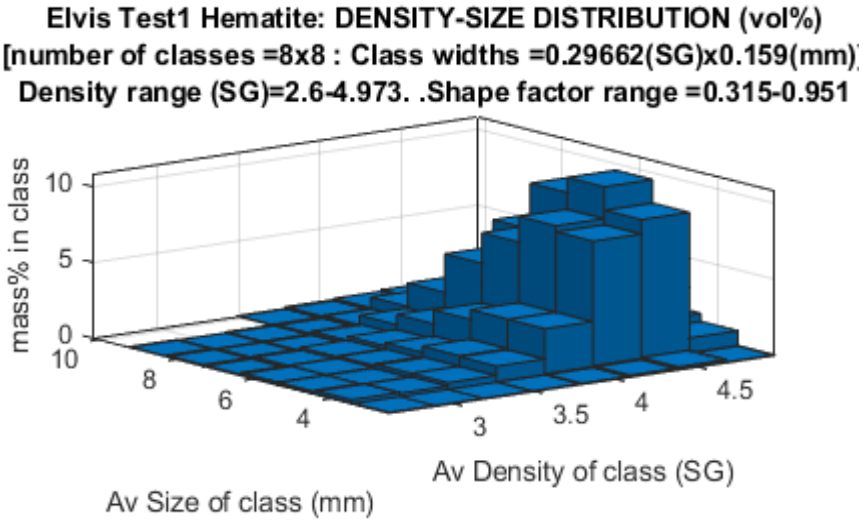


Figure 12: Density-Size 3D distribution.

4.3.2. Partition curve

Partition curves relate the specific gravity of particles to their partition numbers P(i), which are the proportions of those particles that report to either the sinks product or the floats product. The ideal partition curve represents the perfect separation of particles based on their density, where particles with higher densities are separated from those with lower densities. It shows the relationship between particle density and separation efficiency and provides information about other important metrics, such as the cut density and the Écart Probable Moyen (EPM). The cut density, represented by ρ_{50}, is the density at which a particle has an equal chance of reporting to the top or bottom product. On the other hand, the EPM is a measure related to the sharpness of separation. Sharper separations will result in better product grades. The following expression defines the EPM:

$$\text{EPM} = \left|\frac{\rho_{75}-\rho_{25}}{2}\right| \quad \ldots (3)$$

The density of particles that have a 75% and 25% chance of being in the top or bottom product are represented by ρ_{75} and ρ_{25} respectively. The separation is more efficient

when the EPM is lower, meaning the line between ρ_{25} and ρ_{75} is closer to vertical. The EPM can be normalized by dividing it by the cut density to get the imperfection (Ic), which is a normalized measure of separation efficiency

$$I_c = \frac{EPM}{\rho_{50}} \quad \ldots (4)$$

The influence of particle size and shape on jig performance can be conveniently described by how they influence the EPM and the cut density. This influence can be appreciated by observing that a decrease in EPM corresponds to an increase in the sharpness of partition curve and, therefore, on the efficiency of the density separation achieved by the jig. The influence of particle size and shape on EPM and cut density also can be appreciated by the way these two parameters are incorporated in typical partition functions that describe the whole partition curve. This can be seen in Figure 13 below which presents 9 different partition functions that can be used to describe typical partition curves. It was found that expression 3 gave the most accurate fits of the partition data in this study.

Earlier figures demonstrate that the partition numbers can be somewhat erratic, so each curve is modelled empirically by applying a mathematical expression for partition number P(i) vs density rho (i). The table below shows King's options. It was found that Model 3 fitted partition curves significantly better than the other models.

Type	Function	Relationship between I_c and
1	$R(x) = G[\ (1-x)]$	$I_c = 0.674$
2	$R(x) = 1 - G(\ \ln x)$	$I_c = \sinh\ \frac{0.674}{\ }$
3	$R(x) = \frac{1}{1+\exp(\ (x-1))}$	$I_c = 1.099$
4	$R(x) = \frac{1}{1+x}$	$I_c = \sinh\ \frac{1.099}{\ }$
5	$R(x) = \exp(-0.693x\ )$	$2I_c = 2^{1/\ } - 0.415^{1/}$
6	$R(x) = 1 - \exp(-0.693x^{-}\ )$	$2I_c = 2.411^{1/\ } - 0.5^{1/}$
7	$R(x) = \frac{e\ \ -1}{e\ \ +e^{\ x} - 2}$	$2\ \ I_c = \ln\ \frac{9e\ \ -6}{e\ \ +2}$
8	$R(x) = \frac{1}{2} - \frac{1}{\ }\tan^{-1}(\ \ (x-1))$	$I_c = 1.0$
9	$R(x) = \frac{1}{1+\exp(\ \ (x^n-1))}$	$2I_c = \ \ 1+\frac{1.099}{\ }^{1/n} - \ \ 1-\frac{1.099}{\ }^{1/n}$ $2I_c < 2^{1/n}$

Figure 13: Empirical equations for density separations in mineral processing units (King, 2001).

Where $\boldsymbol{x = \frac{\rho}{\rho_{50}}}$

4.4. Influence of particle density on Jig performance

The first research question is addressed in this section, how does the particle's density affect the jig performance? To answer this question performance indicators discussed in section 4.2 are used. The density partition curve describes the effect of the particle density on jig performance. Figure 14 presents all the density partition curves for recovery to the bottom product for samples in Test 1.

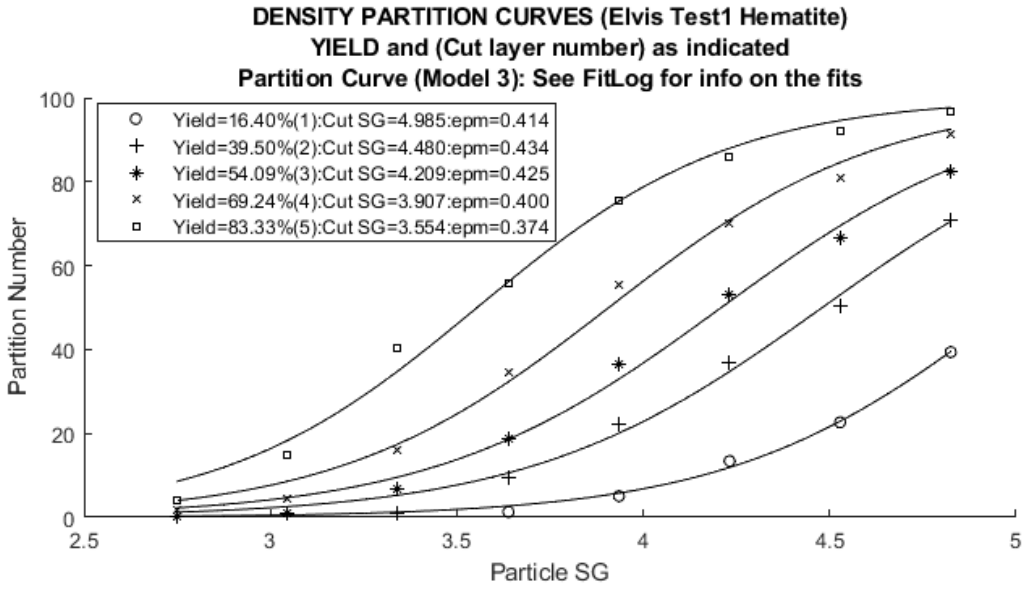


Figure 14: Density partition curve graph.

There is a different partition curve for each cut height i.e., yield, and each partition curve gives a different cut density and EPM. High yield means the bed is cut near the top of the bed, and most of the product is recovered to the sinks product. A 16.4% Yield is obtained by cutting the bed at the top of layer 1. The table below summarises the different percentage yields obtained by cutting the bed at the top of each layer.

Table 3: Percentage yield for cutting the bed at the top of each layer.

Cutting the bed at the top of the Layer	Yield (%)
Layer 1	16.4
Layer 2	39.5
Layer 3	54.09
Layer 4	69.24
Layer 5	83.33

As the bed is stratified, high density materials are recovered in the bottom layer and lower density materials are concentrated near the top of the bed. It is demonstrated in the density partition curve that higher density particles have greater partition number than lower density particles and partition numbers increase with increasing yield.

4.5. Influence of particle size on jig performance

To answer the second research question i.e., how does particle size affect the jig performance, the effect of size on the density partition curve is investigated. The EPM and cut density are used as performance indicators to determine the changes in the partition curve due to different particle sizes. Each figure below shows the density partition curves associated with each percentage yield. Each diagram shows how the partition curve changes with particle size.

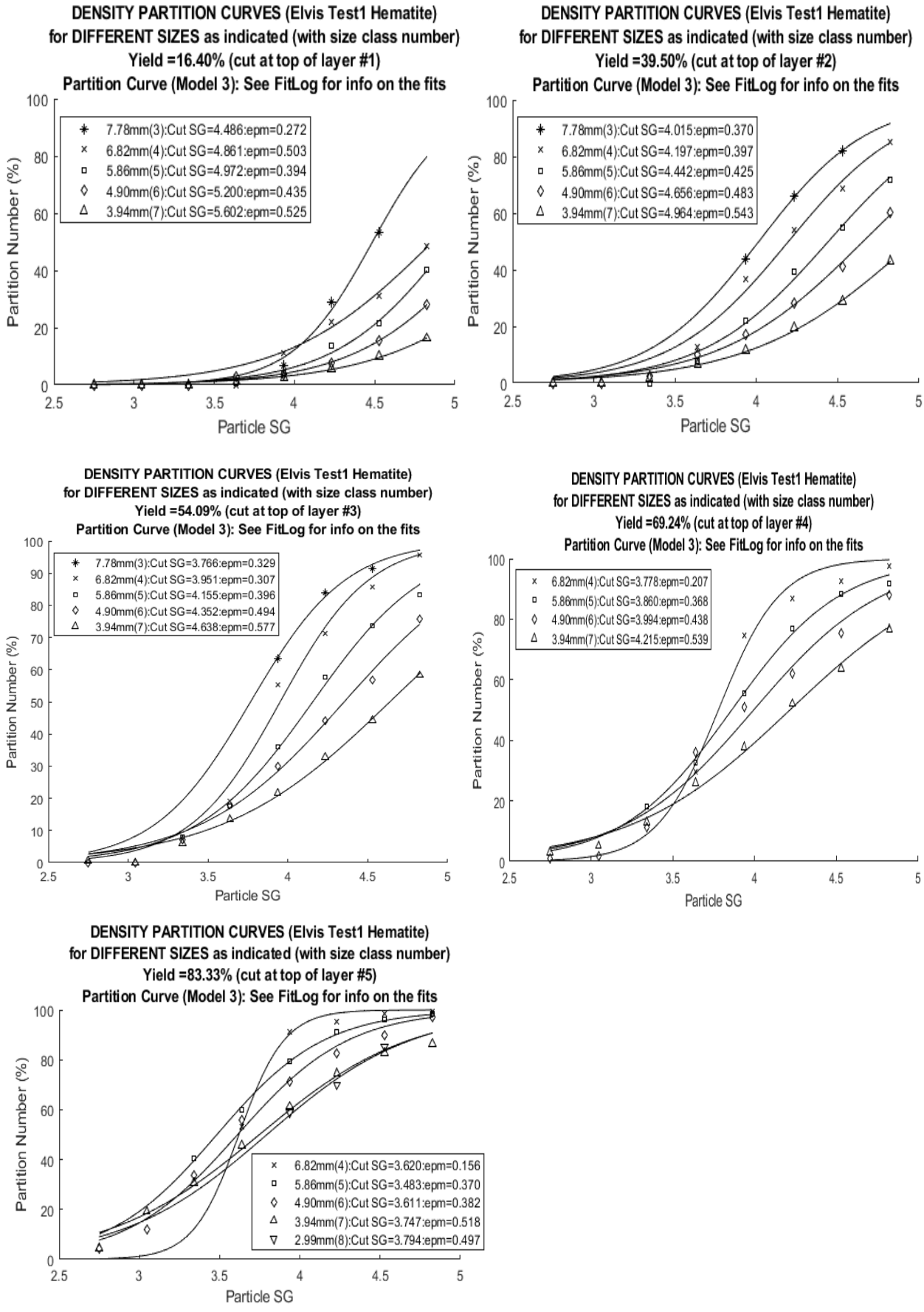


Figure 15: Density partition curves for different particle sizes for different yields.

It can be observed from figure 15 that the particle size has a significant influence on the density partition curve. Each set of partition curves applies to a particular yield and shows the partition curves for each size class at that yield. The sequence of partition curves is such that coarser particles have the larger partition numbers followed by the next smaller size class and so on. Coarser particles have higher partition numbers, hence are recovered more toward the bottom layer of stratification and smaller particles have lower partition numbers and are concentrated near the top layer.

Figure 16 illustrates how particle size hugely affects the density partition of a particle of a given density (in this case, density= 4.231 g/cc). As seen in this diagram, the partition number at a yield of 16.4% can range between 3% and 29% depending on particle size. It varied from 14% to 66% at a yield of 39.5% and 30% to 84% at a yield of 54.09%; at a yield of 69%, it varied between 52% and 93% and at a yield of 83.33% between 70% and 97%. The general observation is that the partition number increases going up the bed; this is because more and more of the bed is removed to the lower product layer.

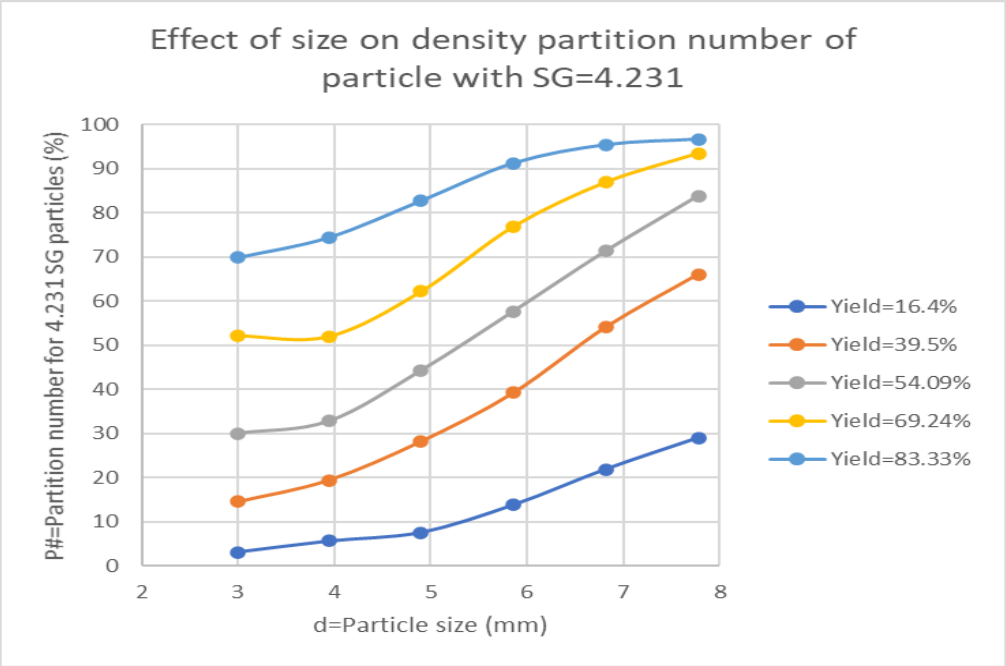


Figure 16: Graph showing the effect of particle size on density partition number of particles with SG=4.231

The effect of particle size on jig performance can be described more precisely by showing its influence on the EPM and cut density associated with each partition curve. This is shown in Figure 17 below. It shows that the influence of particle size on EPM and cut density is reasonably linear. The linear fit equations are shown in the figure, and in Table 4 and 5 where 'm' is the slope and 'c' the intercept in the linear fits.

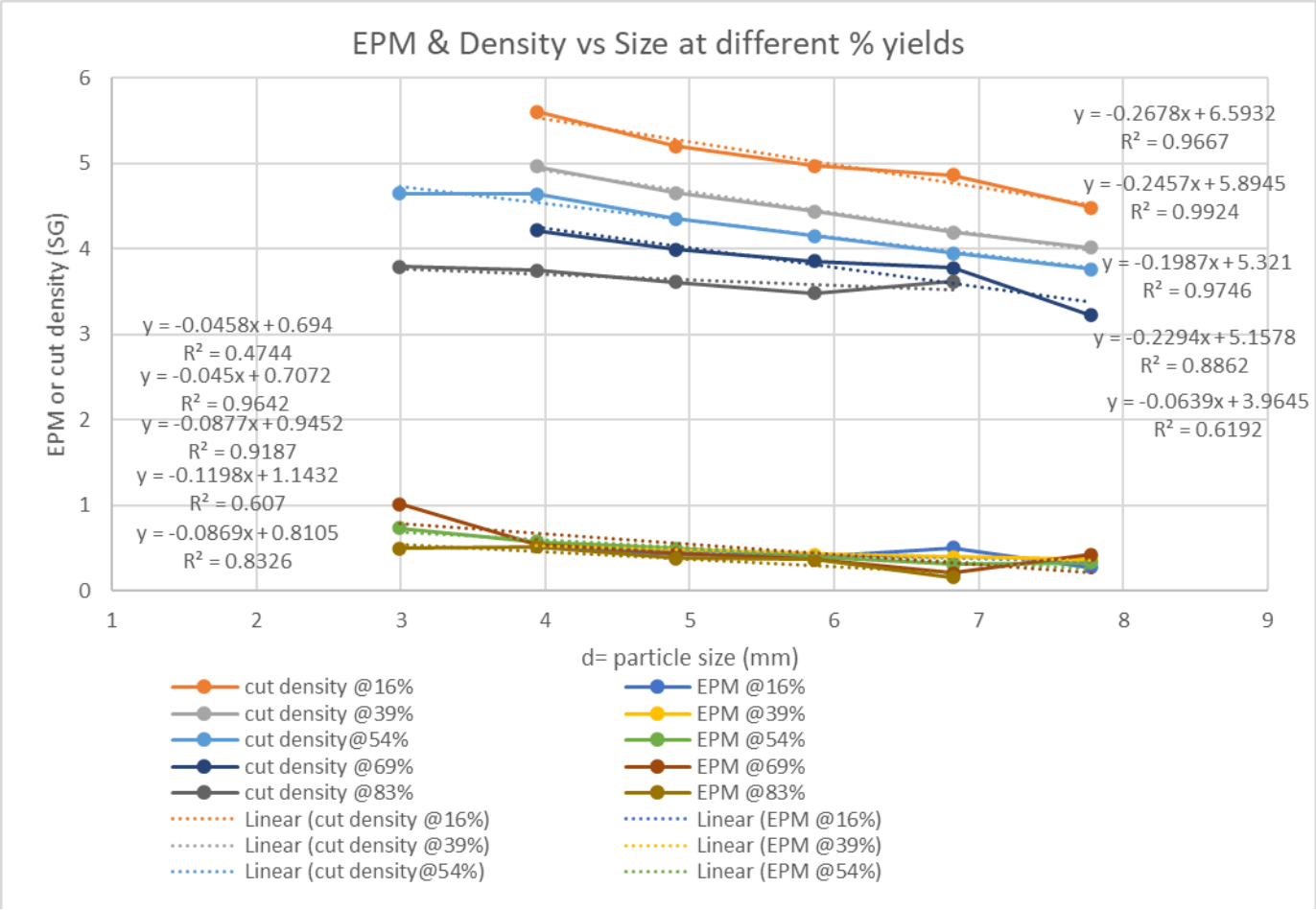


Figure 17: Effect of size on EPM & cut density at different %yield.

Table 4: Linear fit parameters for Cut Density vs Particle size.

Cut density		
Yield (%)	m	c
16	-0.2678	6.5923
39	-0.2457	5.845
54	-0.1987	5.321
69	-0.2294	5.1578
83	-0.0639	3.9645

Table 5: Linear fit parameters for EPM vs Particle size.

EPM		
Yield (%)	m	c
16	-0.0458	0.694
39	-0.045	0.7072
54	-0.0877	0.9452
69	-0.1198	1.1432
83	-0.0869	0.8105

4.6. Modelling the effect of yield and particle size on the partition curves

Figure 17 suggests that EPM may be relatively independent of %Yield if the scatter in the data is attributed to experimental error. It also shows that the cut density is strongly influenced by %Yield. Accordingly, the parameters 'm' and 'c' from the linear fits of cut density vs particle size were plotted against %Yield, Figure 18.

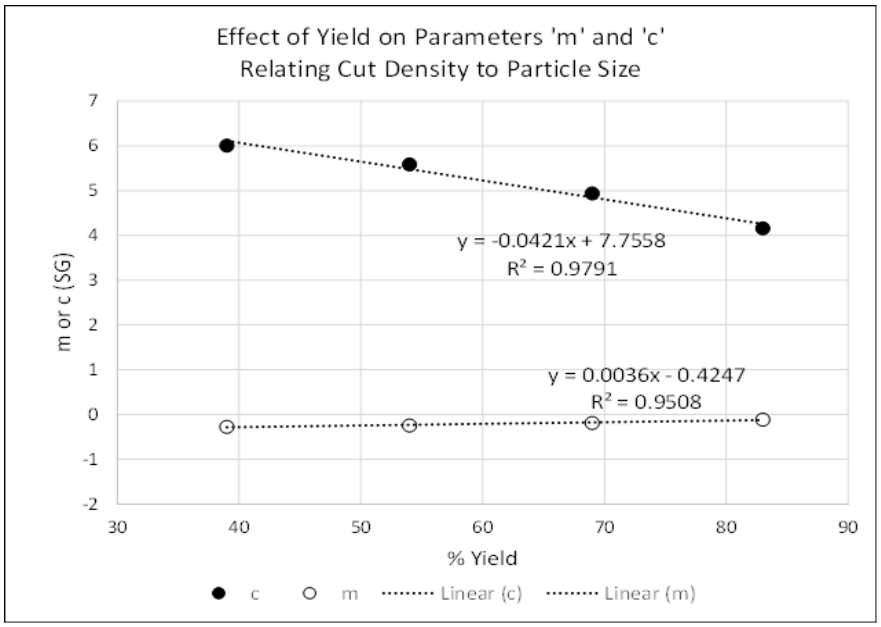


Figure 18: Effect of Yield on the linear fits of Cut density vs Particle size.

The linear fits in Figures 17 and 18 suggest that all the partition curves showing the effect of size on density partition can be described using the Model 3 partition function and the following set of linear equations.

$$\mathbf{EPM\ (SG)} = \mathbf{m_{epm}} \times \mathbf{particle\ size\ (mm)} + \mathbf{c_{epm}} \quad \ldots (5)$$

$$\mathbf{Cut\ Density\ (SG)} = \mathbf{m_{cut}} \times \mathbf{particle\ size\ (mm)} + \mathbf{c_{cut}} \quad \ldots (6)$$

$$\mathbf{m_{cut}\ (SG)} = \mathbf{m_3} \times \mathbf{Yield} + \mathbf{c_3} \quad \ldots (7)$$

$$\mathbf{C_{cut}\,(SG)\;=\;m_4\;\times Yield\;+\;c_4} \qquad \ldots (8)$$

This model has 6 parameters: $\mathbf{m_{epm}}$, $\mathbf{c_{epm}}$, $\mathbf{m_3}$, $\mathbf{c_3}$, $\mathbf{m_4}$, **and** $\mathbf{c_4}$ but includes all the partition data for the effect of all particle densities and all particle sizes.

Professor Woollacott coded the model in MATLAB and fitted it to all the partition data that derived from classes with 50 particles or more. The rationale for this cut off was that partition numbers derived from particle classes with fewer than 50 particles were unreliable and were mostly scattered about the partition curve trend derived from classes that contained 50 or more particles. The sample of fits to partition curves in Figure 19 illustrates this scatter and also shows the high quality of the fits of the model to the partition data for Test 1. The parameter values for the model fit were as follows

m_{epm} = -0.0529 **c_{epm} = 0.736**

m_3 = 0.00177 **c_3 = -0.317**

m_4 = -0.0340 **c_4 = 7.27**

Figure 19 shows an example of fits of the model to the partition data for 12x12x6 classes when cutting the bed at 39.5% yield (at the top of layer 2). The Model fits very well the partition data derived from particle classes with 50 or more particles, as shown by ringed data points. As can be seen, these align very well with the model predictions shown by the solid lines. The 'unreliable' data points, i.e., those from classes with less than 50 particles, are sometimes very scattered, and sometimes reasonably aligned with the model predictions.

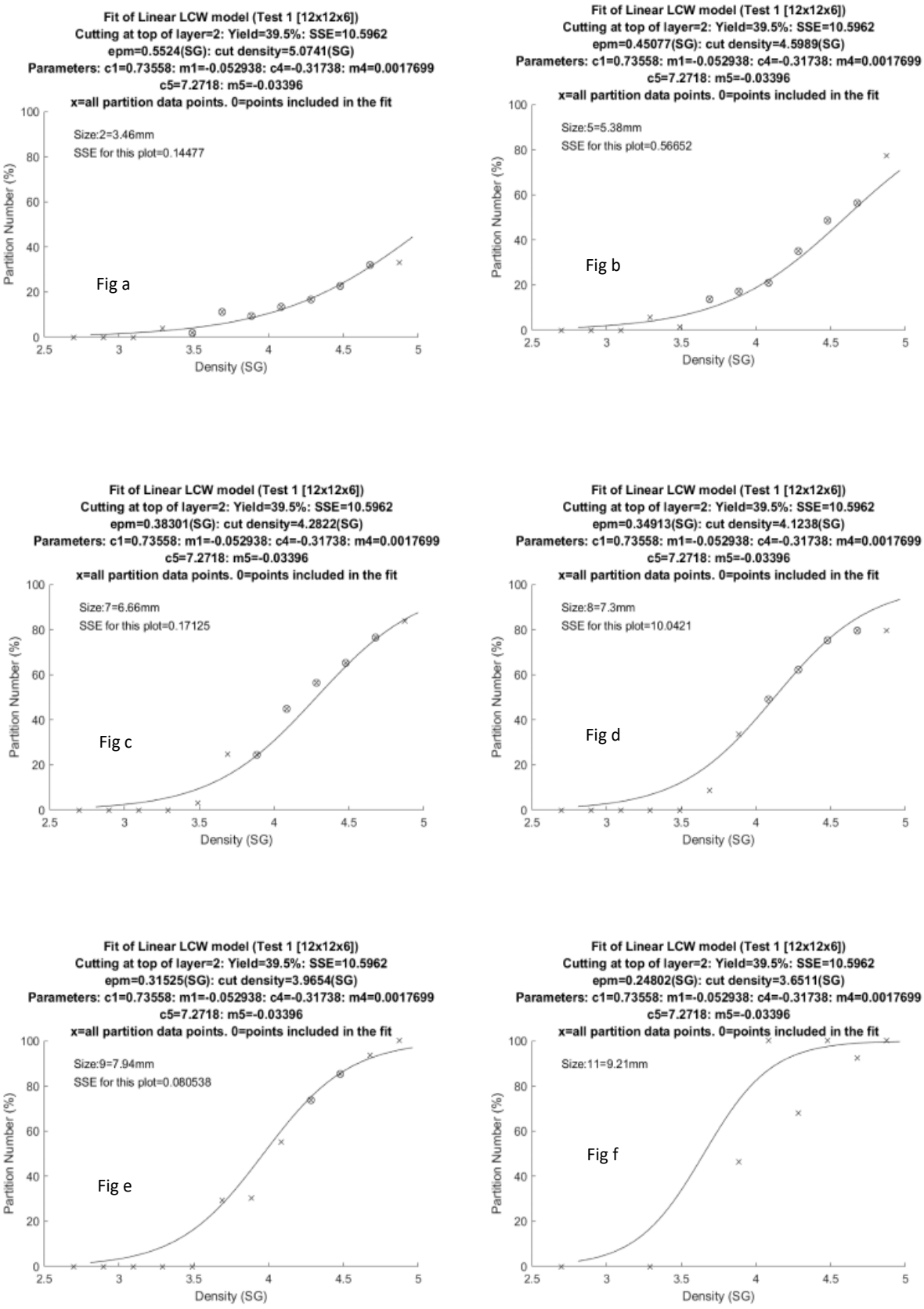


Figure 19: Example of fits of the overall linear model to the partition data. Crosses indicate partition numbers for all data points. Ringed crosses indicate which are 'reliable' because they are derived from classes with more than 50 particles.

4.6.1. Summary of the effect of particle size on jig performance.

The overall trend from the various analyses of the effect of particle size on jig performance is that particle size has a considerable influence on the stratification of particles in the jig. Larger particles tend to settle toward the bottom of the bed, while smaller particles tend to migrate toward the top of the bed, regardless of the percentage yield. It is noticed that the cut density decreases with increased particle size and also decreases as the yield increases; due to the increasing accumulation of smaller and less dense particles as the bed height increases. The EPM discussed in section 4.3.2, is less affected by the particle size as shown clearly in all the yield percentages.

4.7. Influence of particle shape on jig performance

To analyse the effect of particle shape on jig performance, the partition curves depicting the influence of shape are plotted with respect to a particular particle size. The EPM and cut densities derived from the partition curves then provide a means of showing the influence of particle shape on jig performance quantitatively. However, with many size classes, there were insufficient numbers of particles to plot meaningful partition curves. It was only possible to investigate the effect of shape in size classes 5, 6 and 7.

4.7.1. Effect of shape on partition curves for particles in the size class 5 (5.86mm) at different yields.

In size class 5, the partition curve for shape class 1, i.e., shape factor= 0.871, was plotted from only two points, which is insufficient for a reliable partition curve using Model 3. To adequately fit partition curves, there must be three points or more. Hence the partition curve for shape class 1 is removed from the analysis in some of the following graphs leaving partition curves for only shape class 2 and 3 which were fitted from more than 3 points.

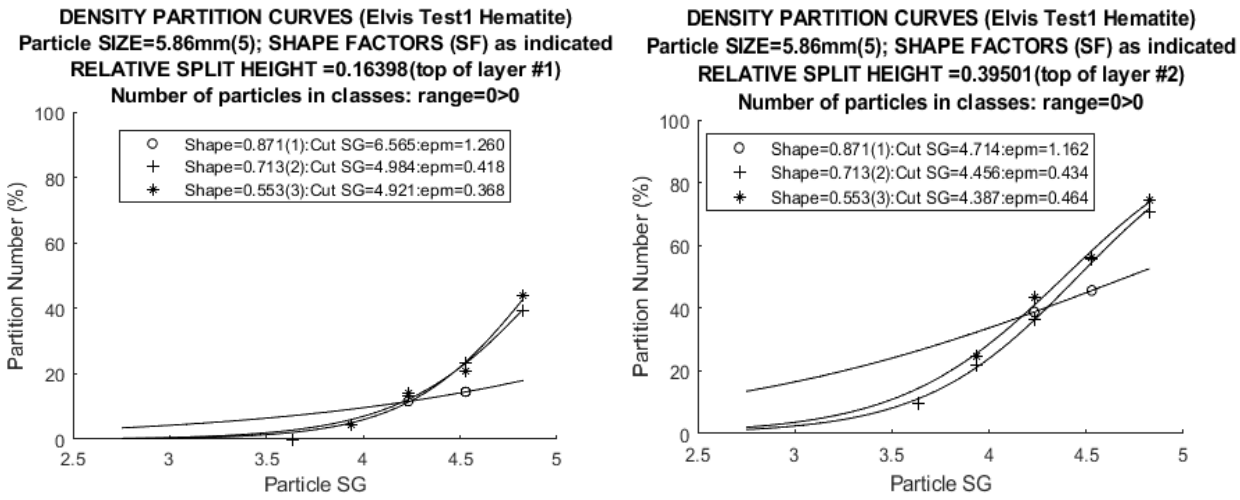


Figure 20: Effect of shape on partition curves for particles in size class 5 with 16% and 39% Yields (i.e., cutting the bed at the top of layers 1 and 2).

Figures 20 and 21 show the effect of shape on density partition curves in particles of size class 5 i.e., 5.86mm. It can be observed that shape has only a small effect on the density partition curve. When cutting the bed at the top of layer 3 and 4 (Yields 54% and 63%), however, there is a noticeable difference in the partition curves for lower density particles (SG<4.3) between shape factor 2 and 3, where the flatter particles (shape 3) tend to have higher partition numbers, meaning they are reporting more to the bottom layer. This is the opposite of what one would expect. One would expect the flatter or more elongated particles to settle more slowly than less flat particles and so would tend to report more to the top layers.

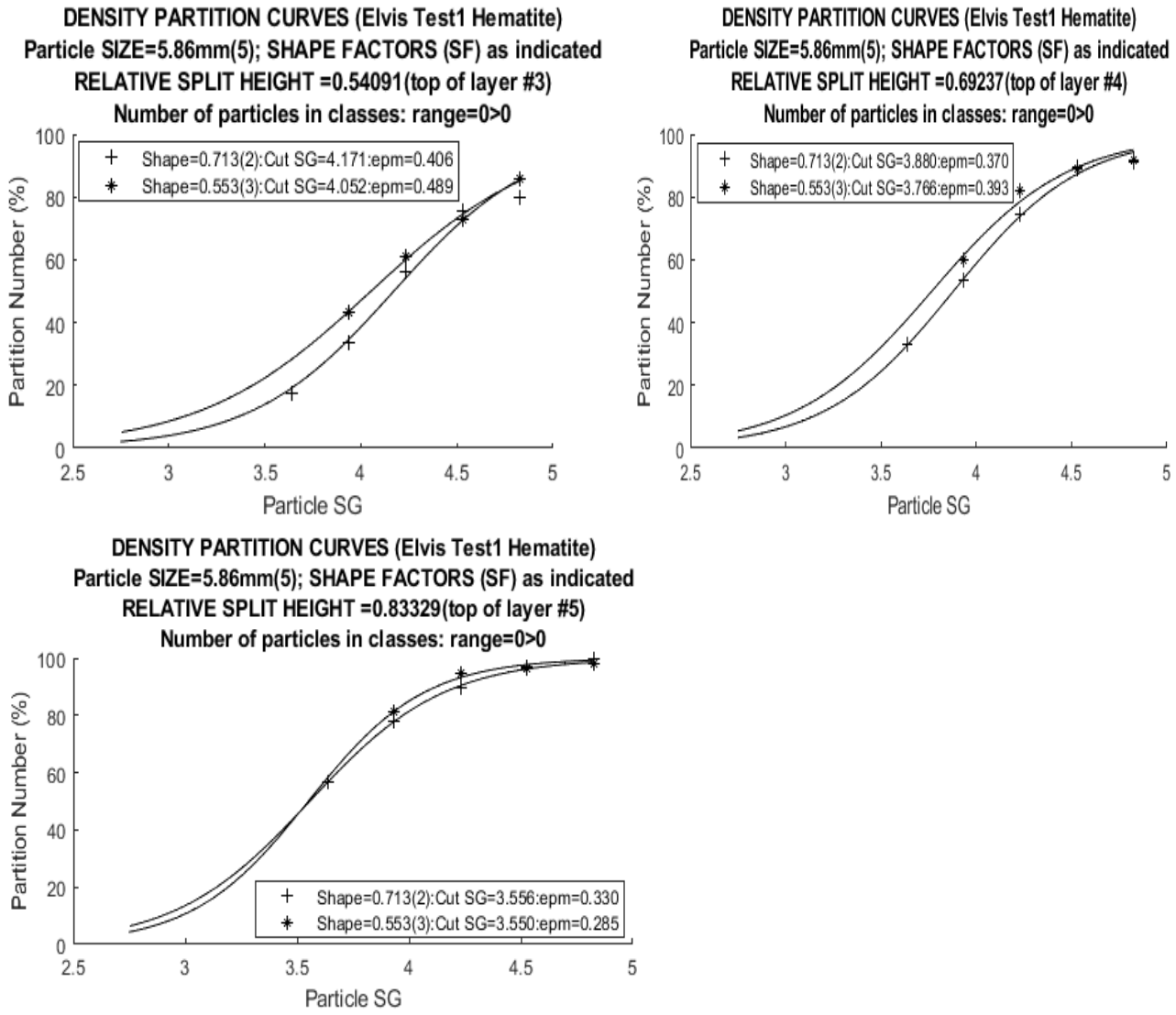


Figure 21: Effect of shape on partition curves in size class 5 (5.86mm) with 54%, 69% and 83% Yields (i.e., cutting the bed at the top of layers 3, 4 and 5).

4.7.2. Effect of shape on partition curves for particles in size class 6 (4.9mm) at different yields.

Figure 22 shows the effect of shape on density partition curves in size class 6 (4.9mm) for yields from 16 to 83%. These are all well-defined partition curves. The same unexpected effect of shape noted for size class 5 is also evident in size class 6. The flatter, more elongated particles seem to concentrate in layers lower than the more spherical or cubic-shaped particles; and so, have higher partition numbers.

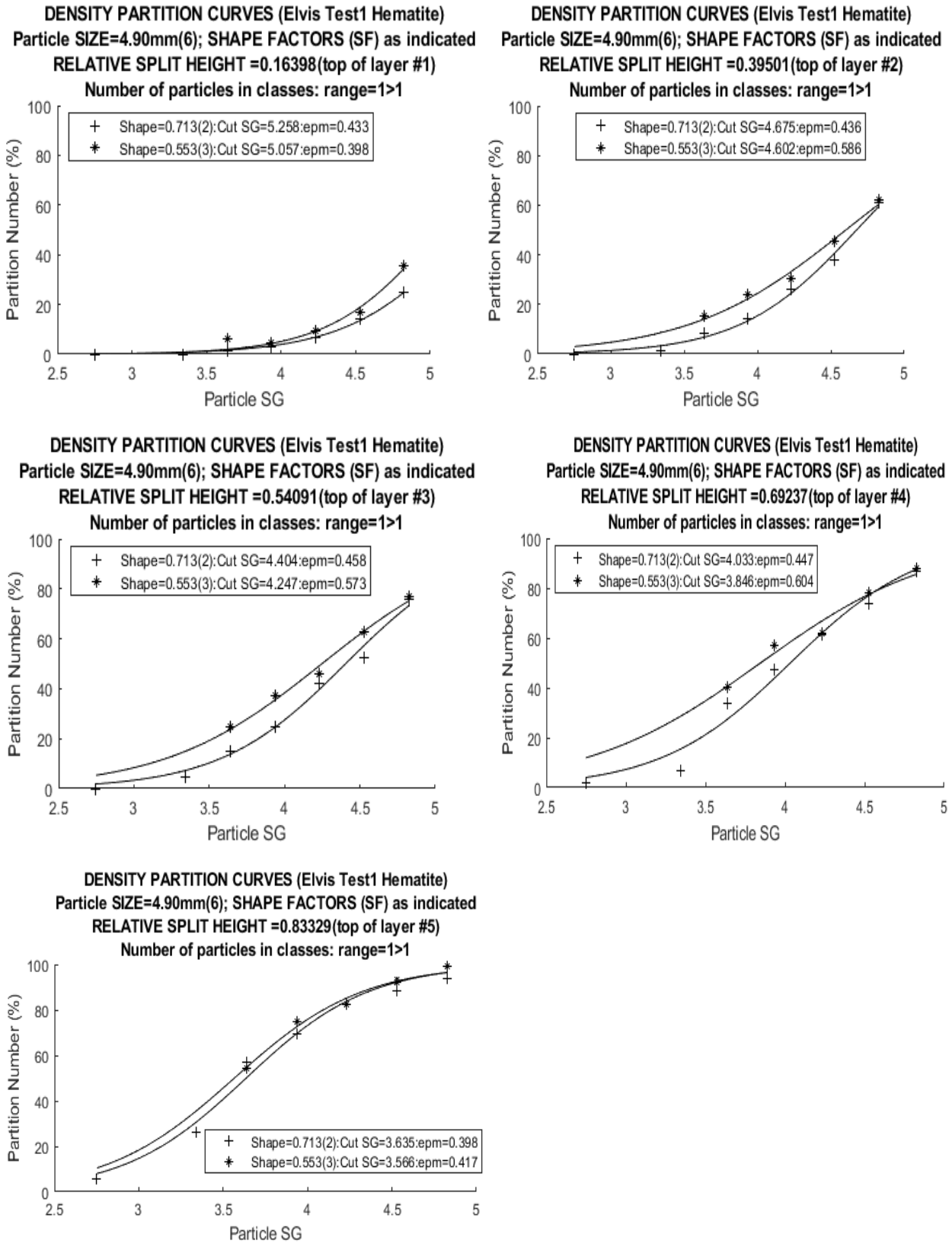


Figure 22: Effect of shape on density partition curves for size class 6 (4.9mm) particles for different yields.

4.7.3. Effect of shape on partition curves for particles in size class 7 (3.94mm) at different yields.

Figure 23 shows the effect of shape on density partition curves in size class 7 for yields from 16 to 83%. Again, the partition curves are well defined. In Layer 1 (16% yield), the partition curves for differently shaped particles overlap, probably due to the effect of size as size class 7 consists of particles with small size (3.94mm). As such they tend to concentrate in upper layers on the jig bed. For yields 39, 54 and 69%, the same unexpected trend noted before is evident. The flatter, more elongated particles have higher partition numbers than the more cubical or spherically shaped particles. For an 83% yield the trend is still there but less pronounced, probably because, following the previous argument, the more spherical or cubically shaped particles are more concentrated at the top of the bed.

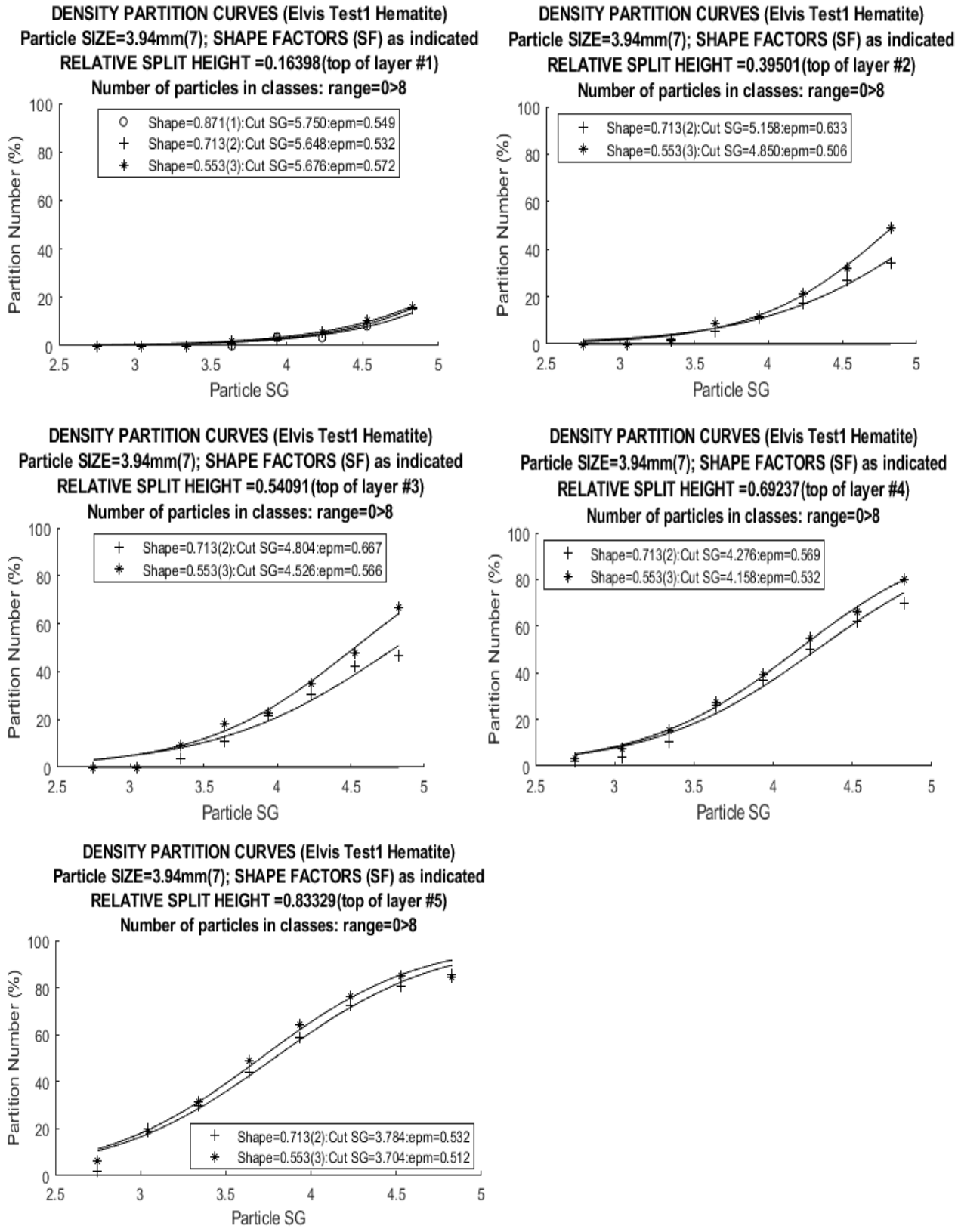


Figure 23: Effect of shape on density partition curves in size class 7 (3.94mm) for different yields.

4.7.4. Evaluation of particle shape effect on cut density and EPM as cut height increases.

Figures 24, 25 and 26 show the EPM and cut densities for partition curves for each size and yield. There seem to be anomalies in the EPM and cut density data that obscure the general trends in the three figures. The trend is that shape factor seems to have little influence on EPM and cut density, as Figure 25 suggests. If apparent anomalies are ignored, each plot seems flat indicating the same EPM or cut density over the range of particle shapes. In Figure 24 the EPM for shape factor 0.871 seem high at 16 and 39% yield. And cut density for shape factor 0.871 seems high at 16% yield. In figure 26 the EPM and cut density for 39% yield seem high.

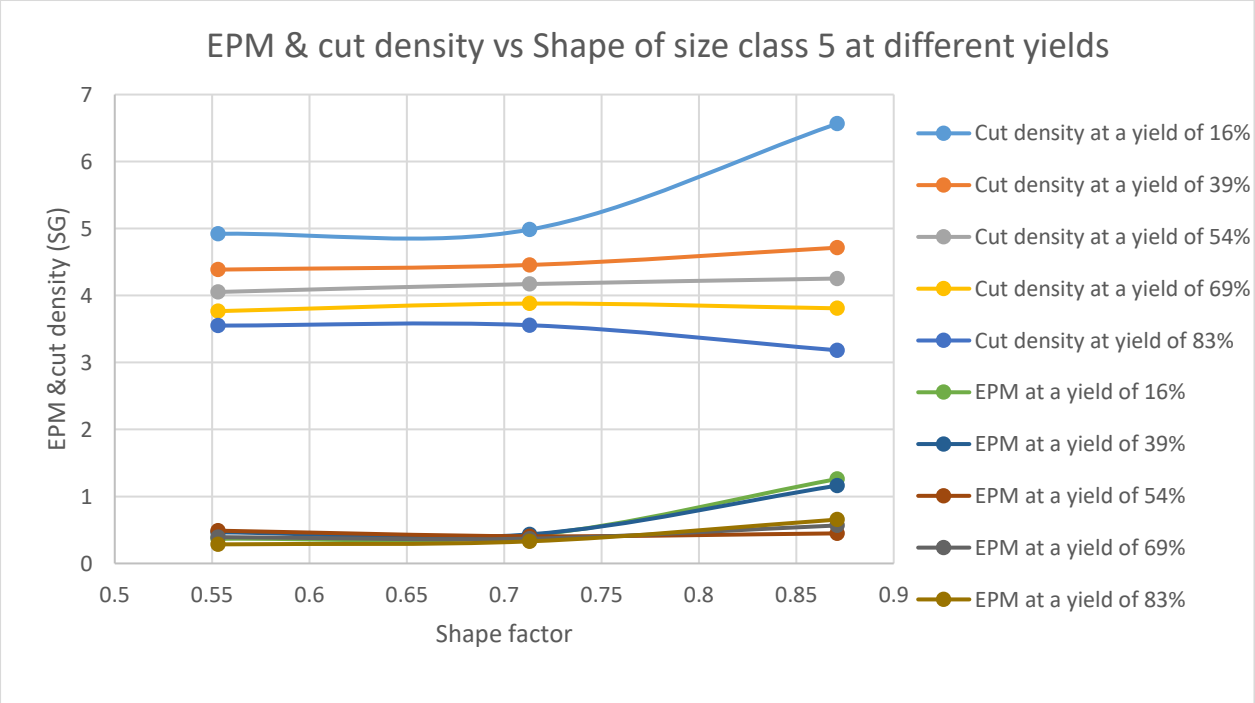


Figure 24: Effect of shape on EPM and cut density in size class 5 at different yields.

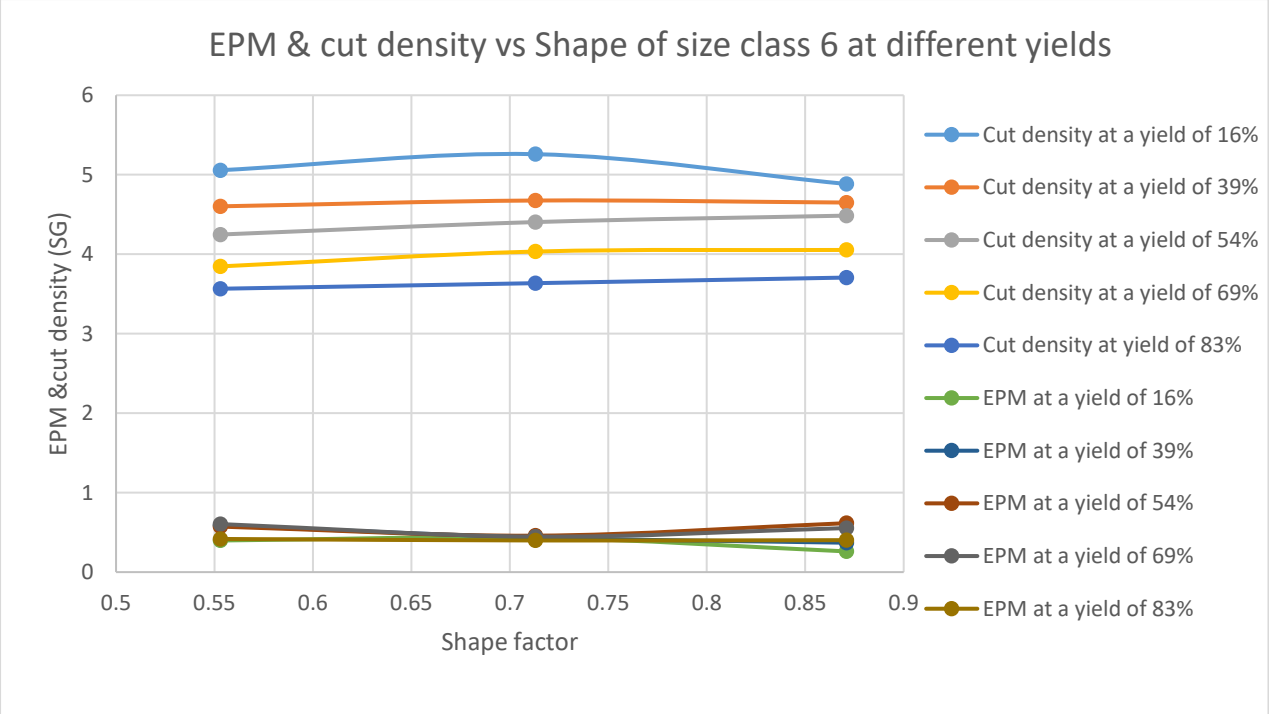


Figure 25: Effect of shape on EPM and cut density in size class 6 at different yields.

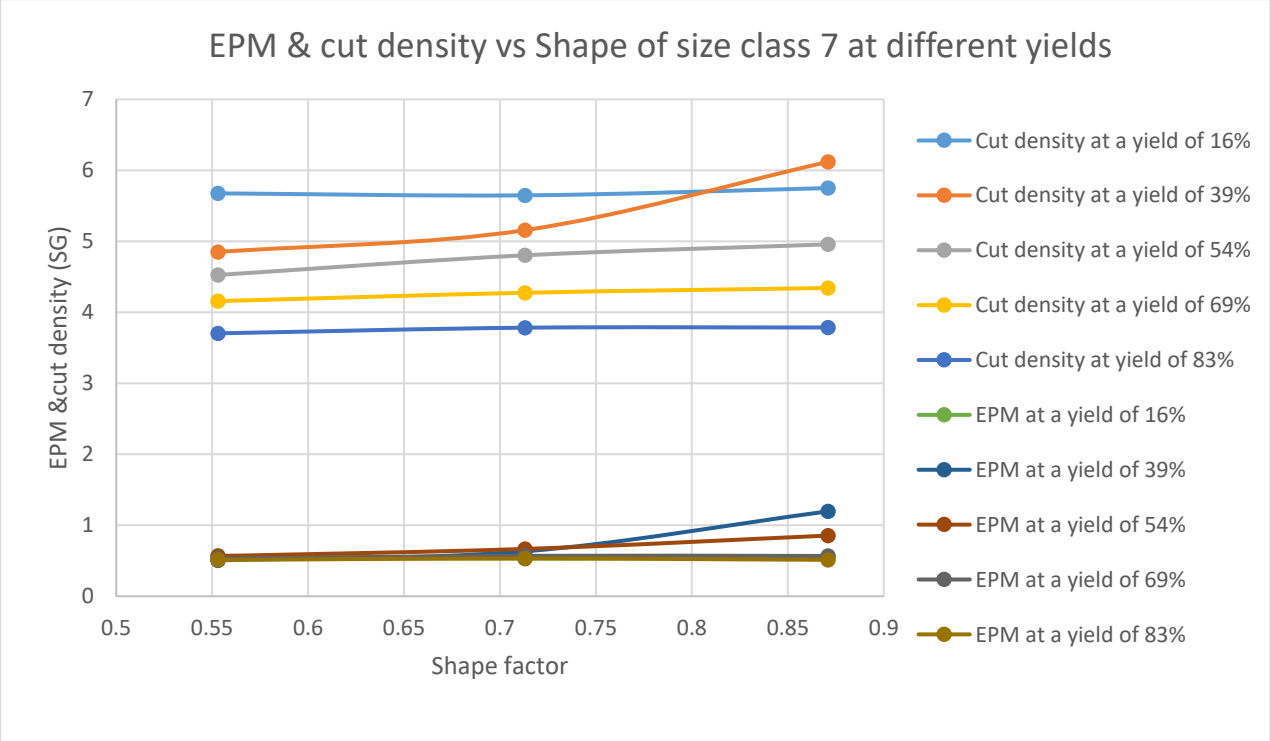


Figure 26: Effect of shape on EPM and cut density in size class 7 at different yields.

4.7.5. Summary of the effect of shape on cut density and EPM

The effect of shape on cut density and EPM is not as clear or as prominent as was suggested by the observations made from the partition curves in sections 4.7.1 to 4.7.3. It appears that the shape of particles does not have a significant impact on the cut density and EPM. It may be that the effect noted from the partition curves is not revealed by this analysis because (1) the effect is small, (2) because the data may have some experimental error and fitting error, (3) because the analysis is trying to show the effect on two metrics, EPM and cut Density, and (4) because each trend is defined by only 2 or 3 data points. There does not appear to be any particular pattern to the anomalies or deviations from the general trends. Therefore, another approach is taken to analyse the effect of shape on stratification that was suggested from the previous analysis on partition curves. The influence of particle shape on that data is now analysed by plotting the partition numbers for different shape factors for particles with the same size and density; partition data are plotted for size classes 5 (5.86mm), size class 6 (4.9mm) and size class 7 (3.94mm) and for density classes 1 (4.825 g/cc), density class 2 (4.528g/cc), density class 3 (4.231g/cc) and 4 (3.935g/cc).

4.7.6. Effect of shape on partition numbers

Figures 27, 28 and 29 show the influence of shape on the partition numbers for particles with specific density and size. There are much fewer anomalies in these diagrams and the trends seem to be more consistent. Those trends are that the partition numbers either do not change as the shape factor increases, or, more usually, they decrease a little. The decrease is not very large but appears to be consistent.

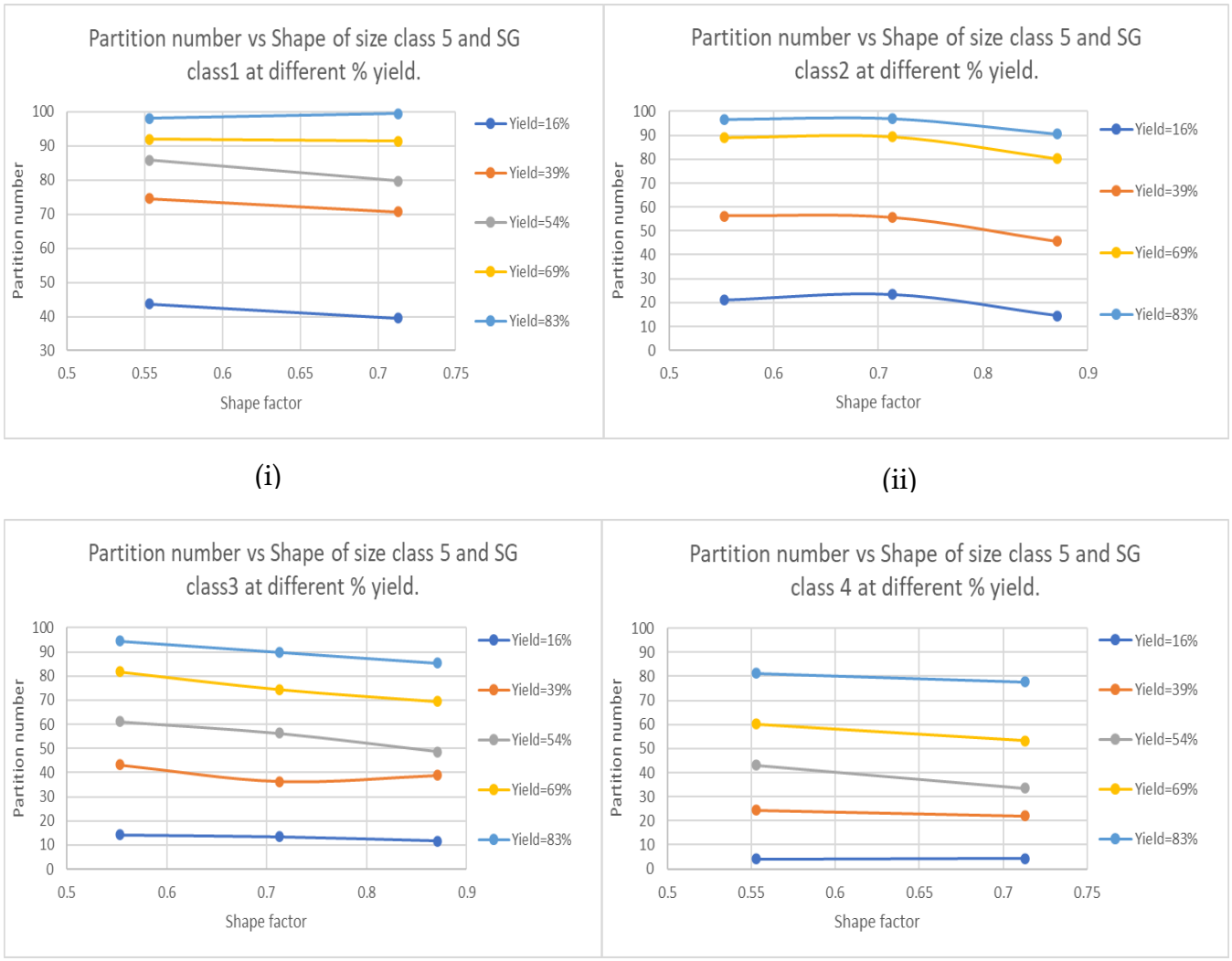
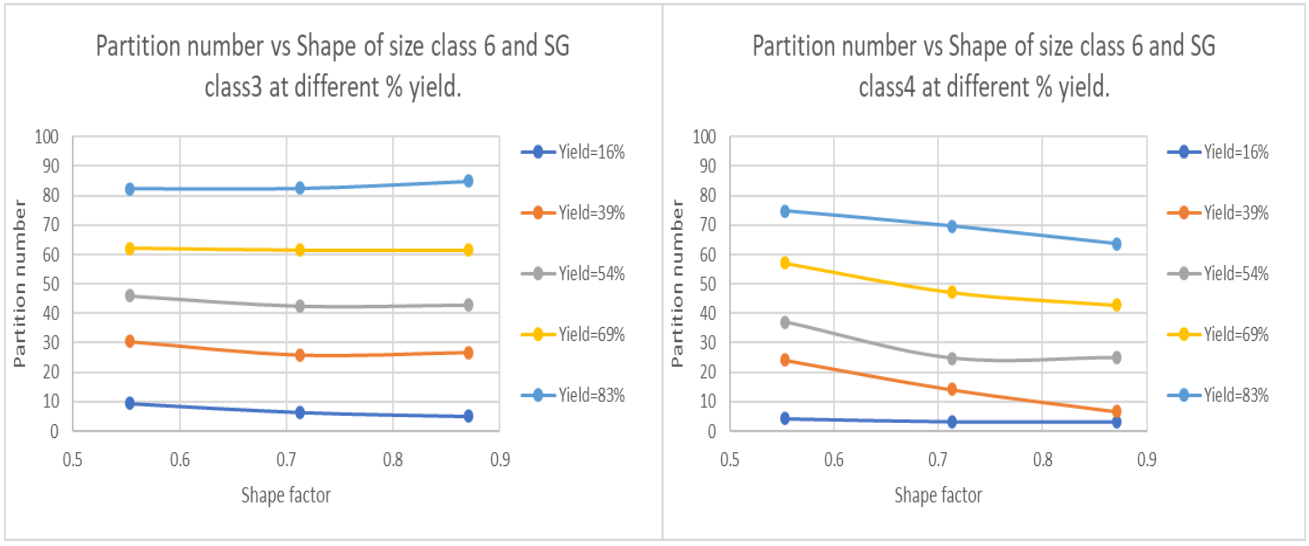


Figure 27: Effect of shape on size class 5 (5.86mm) and (i) SG class 1; (ii)SG class 2; (iii) SG class3; (iv) SG class 4 at different yields.



(i)

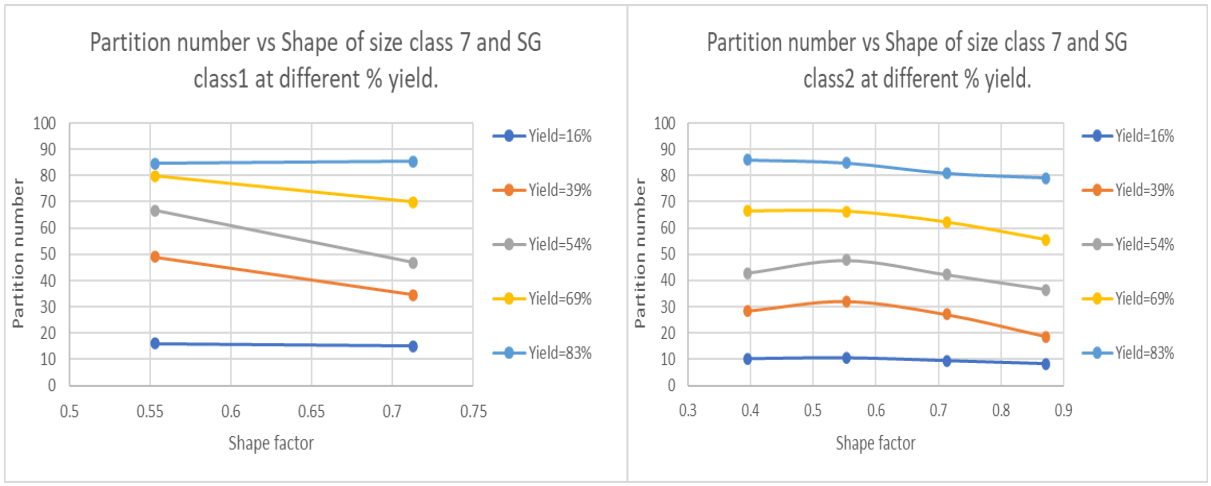
(ii)



(iii)

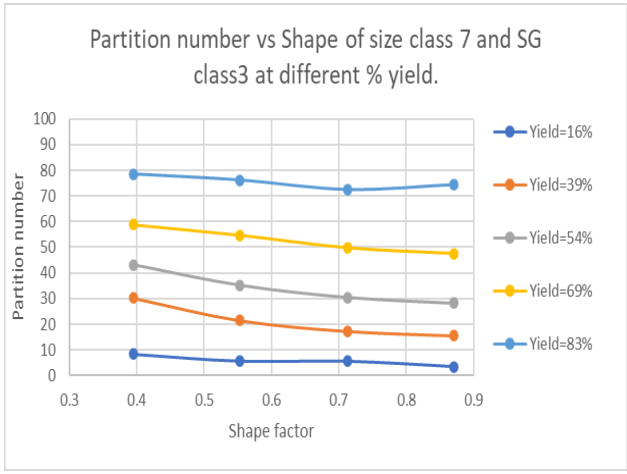
(iv)

Figure 28: Effect of shape on size class 6 (4.96mm) and (i) SG class 1; (ii)SG class 2; (iii) SG class3; (iv) SG class 4 at different yields.

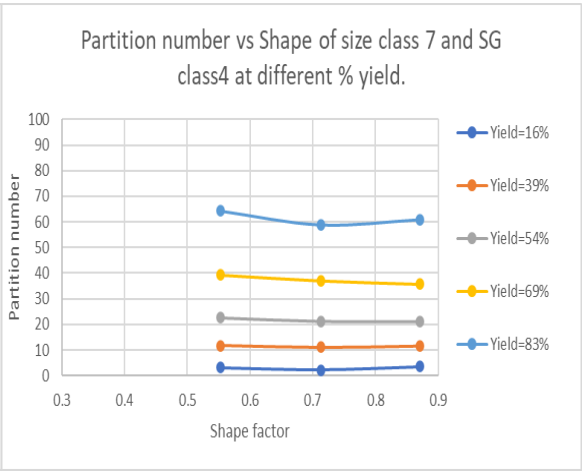


(i)

(ii)



(iii)



(iv)

Figure 29: Effect of shape on size class 7 (3.94mm) and (i) SG class 1; (ii)SG class 2; (iii) SG class3; (iv) SG class 4 at different yields.

4.7.7. Summary of findings on the effect of shape on stratification

The influence of particle shape on the stratification noted from the analysis of the partition curves is revealed more clearly by the diagrams in section 4.7.6. Flatter, more elongated particles have higher partition numbers and report more to the bottom product layer while more spherical or cubic-shaped particles have lower partition numbers and tend to report more to the upper product layer. The influence is not as marked as the influence of size on partition numbers (shown in section 4.5 and figure 16). Also, the effect is not as clearly evident and is not the same for all the data analysed; there are some anomalies from the trends that are observed.

Those trends are as follows. The primary influence is that the partition number seems to increase as the particle shape becomes flatter and more elongated. This suggests that the flatter and more elongated particles penetrate more deeply down into the bed than do the more spherical and cubical particles. As mentioned before this is counter intuitive because flatter more elongated particles tend to settle in water less rapidly than do more spherical and cubical particles. The implication is that in the very hindered settling conditions within a crowded jig bed, it is not so much the fluid resistance that affects the way particles of different shape migrate in the bed, but the ease with which they can slip through the crowded particle bed. More rounded particles seem to have more resistance to downward movement than do elongated or flatter ones that can perhaps slip between particles more easily than the more rounded ones. The second trend noted is that larger particles appear to show this effect more than smaller particles, perhaps because their masses are greater.

Chapter 5: Discussion and conclusion

5.1. Discussion

The study investigated the effect of the density, size and shape of iron ore particles on jig performance. A sample of hematite ore was used for this investigation and the experimental data obtained after jigging was processed by a program written in MATLAB. The following four research questions were asked to investigate the influence of each of the feed property.

Question 1. How does the particle's density affect jig performance?

To study the effect of particle density on jig performance, partition curves were analysed. The results showed that high density particles have higher partition numbers, because they are concentrated more toward the bottom layers of the bed after stratification. That trend was observed throughout the bed with all percentage yields. It was also found that the cut density decreased with increasing cut height. This can be explained by the fact that the number of lighter particles increases going up the bed, therefore the cut density is reduced.

Question 2. How does particle size affect jig performance?

The effect of particle size on separation efficiency was analysed by looking at (1) the influence of particle size on density partition curves for particles of different sizes and (2) the influence of particle size on performance indicators derived from the partition curves, namely the cut density and EPM. It was found that size affected partition curves for all percentage yields, coarser particles had higher partition numbers and finer particles had lower partition numbers. As seen with particle density this indicates that coarser particles tend to report to the bottom layer of the bed and finer particles to the top product layer. This implies that the size of particles influenced the separation, hence the jig performance. The EPM, which is a metric for the sharpness of separation, was not much affected by the size of particles, whereas the cut density decreased with increasing particle size. The explanation here is more complicated because both the size and density of the particles need to be taken into account. It is easiest to explain by assuming that it is the settling rate of particles that determine

how they stratify. Therefore, particles with a 50-50 chance of reporting to the lower layer must have the same settling rate in the jig bed. As a result, a particle of higher density will be smaller than one of lower density that has the same settling rate.

Question 3. How does particle shape affect jig performance?

The effect of particle shape on separation efficiency was investigated in three ways: examination of the partition curves for particles of the same size but different shapes; examination of the EPMs and cut densities from those partition curves; and examination of the effect of shape on the partition numbers of particles with the same density and size. Only three size classes could be analysed, namely, size class 5, size class 6 and size class 7 which represented respectively particles of size 5.86mm, 4.90mm and 3.94mm. In general, the effect of particle shape was surprisingly small. In some cases, there was no effect. It was noticed that particle shape appeared to have some impact on stratification in that flatter, more elongated particles tended to have higher partition numbers which means they were reporting more toward the bottom layer of the bed, while more rounded particles had a lower partition number, implying that they were reporting more towards the top layer of the bed. This effect of shape observed on jig performance must be due to the hindered settling conditions within the jig bed, and the way the particles affect each other. It cannot be the result of differences in the resistance which fluid makes with particles of different size. If it were, then the flatter, more elongated particles would settle more slowly in the jig and would tend to report more to the upper layers than more rounded particles. The partition curves that showed the effect of particle shape, had the same density and size of particles. Therefore, apart from the difference in shape, the particles should have the same settling rate and stratify in a similar way. However, because it has been found that the flatter more elongated particles tend to concentrate more towards the bottom of the bed, it must be that this shape is able to penetrate more deeply into the bed than more rounded particles. This suggests that the movement of particles through the bed as it is consolidating, is easier if the particle has a narrower dimension. Since the effect of shape was analysed by considering different particle sizes independently, it was observed that this shape effect was more pronounced in

coarser particles (5.86mm) than in finer particles (3.94mm) probably due to their larger mass.

Question 4. What are the practical implications of the findings?

The findings in this study shows that stratification in jig is affected by other particle properties such as size and shape. Although, the determining parameter for gravity separation is the density of the material, the size and shape of particles need to be considered for an efficient separation.

5.2. Limitations of the study

The laboratory experiment presented in this report was conducted using a batch jig. All the results and analysis of particles stratification are based on the condition in a batch jig, whereas most mineral processing industries use a continuous jig in which the separation achieved is influenced by other factors as well as stratification. For example, it is affected by the transport rates through the jig where the lower layers in the jig move through the jig more slowly. In addition, there is a degree of remixing of the stratified layers when the layers are split from the jig bed. The findings of this study relate only to stratification in a jig.

5.3. Conclusion

As reported in chapter two of this report, many researchers previously only focused on studying the effect particles density and size on jig performance. This research report contributed in the field by studying the effect of particle density, size and shape of an iron ore. The effect of particle shape has not been investigated previously in detail. It was found that the effect of particle shape on jig performance is counter intuitive in that flatter more elongated particles tend to concentrate mostly toward the bottom of the bed and more rounded particles are concentrated toward the upper layers of the bed after stratification.

RhoVol was used for the first time to determine the effect of particle density, size and shape on the stratification of an iron ore as a result, a program code was developed to read RhoVol data and measurement in a meaningful way.

Though the study was an academic experiment, it was able to develop a model that could be used to predict stratification in a jig bed quite reasonably. It shows the effect of size and yield on partition curves and performance indicators. This is a contribution in the modelling of stratification and a tool that can be used at industrial level to achieve practical results.

References

Ambrós, W. (2020). Jigging: A review of fundamentals and future directions. *Minerals, 10*, 998.

Bosman, J. (2007). Jigging or dense medium separation—which is the best? In: Proceedings Iron. *The Australasian Institute of Mining and Metallurgy*, 225–233.

Brozek, M. & Surowiak, A. (2007). Effect of Particle Shape on Jig Separation. *Physicochemical Problems of Mineral Processing, 41*, 397–413.

Burt, R. (1999). The role of gravity concentration in modern processing plants. *Minerals Engineering, 12*, 1291–1300.

Falconer, A. (2003). Gravity separation: Old technique/new methods. *Physical Separation in Science and Engineering, 12*, 31–48.

Fofana, M. & Steyn, T. (2018). Monitoring the performance of DMS circuits using RhoVol technology. *Journal of the Southern African Institute of Mining and Metallurgy, 119*, 133.

Forbes, K., Voigt, A. & Bodika, N. (2003). Using silhouette consistency constraints to build 3D models. *Proceedings of the Fourteenth Annual Symposium of the Pattern Recognition Association of South Africa* (pp. 33–38). (PRASA 2003).

Jinnouchi, Y., Kita, S., Tanaka, M. & Sawada, Y. (1984). New trends in theory and technology of air-pulsated jigs in Japan. *Minerals and Metallurgical Processing, 1*, 76–81.

Karantzavelos, G.E., Frangiscos, A.Z. (1984). Contribution to the Modelling of the Jigging Process. *Society of Mining Engineers*, 97–105.

King, R. (2001). *Modeling and Simulation of Mineral Processing Systems.* Oxford: Butterworth-Heinemann.

Maré,E.,Beven,B.,Crisafo,C. (2015). Developments in nonmagnetic physical separation technologies for hematitic/goethitic iron ore. *Mineral.Proc.Environ.Sustainability-IronOre*, 309–338.

Mayer.F. (1964). Fundamentals of a potential theory of the jigging process. *Proceedings 7th International Mineral Processing Congress. 1*, pp. 75–86. New York: Gordon and Breach.

Mehrotra, S.P. & Mishra, B.K. (1997). Mathematical modeling of particle stratification in Jigs. *Proceedings of the National Seminar on Processing of Fines* (pp. 202–217). Jamshedpur: NML Jamshedpur.

Mukherjee, A.K. & Mishra, B.K. (2006). An integral assessment of the role of critical process parameters on jigging. *International Journal of Mineral Processing, 81*, 187–200.

Naudé, N., Lorenzen, L., Kolesnikov ,A., Aldrich, C. & Auret, L. (2013). Observations on the separation of iron ore in a prototype batch jig. *International Journal of Mineral Processing, 120*, 43–47.

Pita, F. & Castilho, A. (2016). Influence of shape and size of the particles on jigging separation of plastics mixture. *Waste Management, 48*, 89–94.

Rao, B. (2007). Extension of particle stratification model to incorporate particle size effects. *International Journal of Mineral Processing, 85*, 50–58.

Richards & Jones, T. (2004). The Kelsey centrifugal jig _ an update on technology and application. *SME Annual Meeting* (pp. 4–21). Denver: Society for Mining, Metallurgy and Exploration.

Tavares, L. (1999). Monte Carlo Simulations on the Potential Energy Theory of Jigging. *Coal Preparation, 20*, 71–83.

Tavares, L.M. & King, R.P. (1995). A Useful Model for the Calculation of the Performance of Batch and Continuous Jigs. *Coal Preparation, 15*, 99–128.

Wills, B.A. & Finch, J.A. (2016). *Wills' Mineral Processing Technology* (8th ed.). Oxford: Butterworth-Heinemann.

Woollacott, L.C & Silwamba, M. (2016). An experimental study of size segregation in a batch jig. *Minerals Engineering, 94*, 41–50.

Appendices

Appendix A: Data used to plot the effect of size on EPM & cut density at different % yield (Figure 17).

Table 6: Table showing the influence of size on EPM and cut density at 16% yield.

16% Yield		
Size class	rho50	EPM
7.78	4.486068	0.271543
6.82	4.861138	0.502928
5.86	4.971758	0.393993
4.9	5.200066	0.435262
3.94	5.601809	0.525088

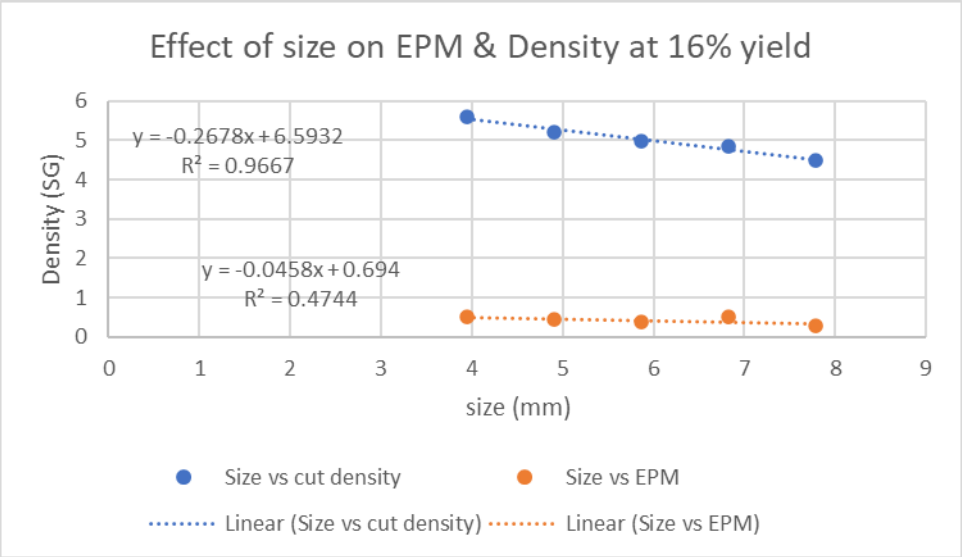


Figure 30: Effect of size on EPM and cut density at 16% yield.

At a yield of 16%, the cut density decreases from 5.6 SG to 4.5 SG as the size increases, while EPM slightly decreases as particle size increases.

Table 7: Table showing the influence of size on EPM and cut density at 39% yield.

39% Yield		
Size class	rho50	EPM
7.78	4.01473	0.36957
6.82	4.196973	0.397363
5.86	4.442427	0.424565
4.9	4.656046	0.483393
3.94	4.964412	0.542551

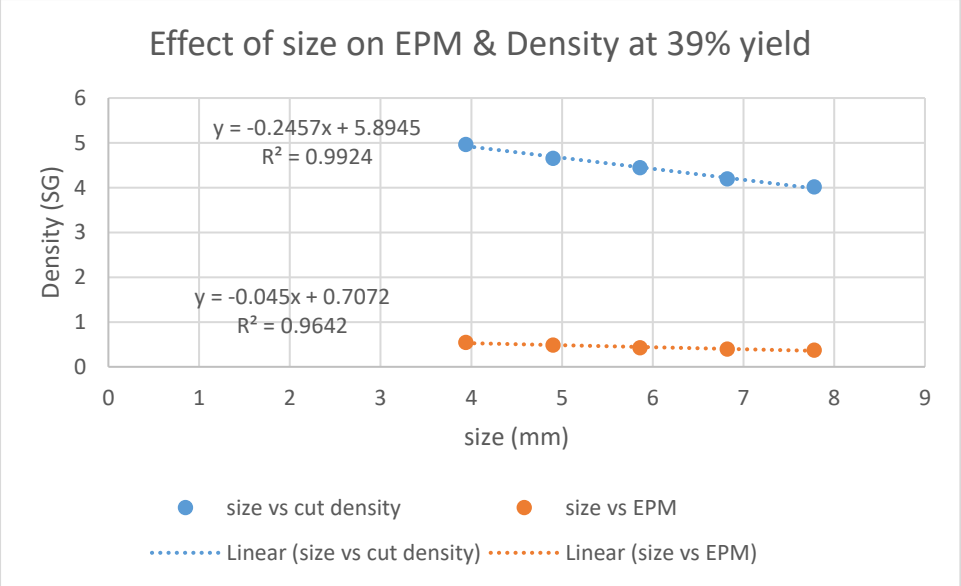


Figure 31: Effect of size on EPM and cut density at 39% yield.

At a yield of 39%, the cut density decreases as the size increases, while EPM slightly decreases as particle size increases.

Table 8: Table showing the influence of size on EPM and cut density at 54% yield.

54% Yield		
Size class	rho50	EPM
7.78	3.765978	0.328565
6.82	3.951226	0.307167
5.86	4.155188	0.3962
4.9	4.351997	0.493849
3.94	4.637744	0.576757
2.99	4.647704	0.736102

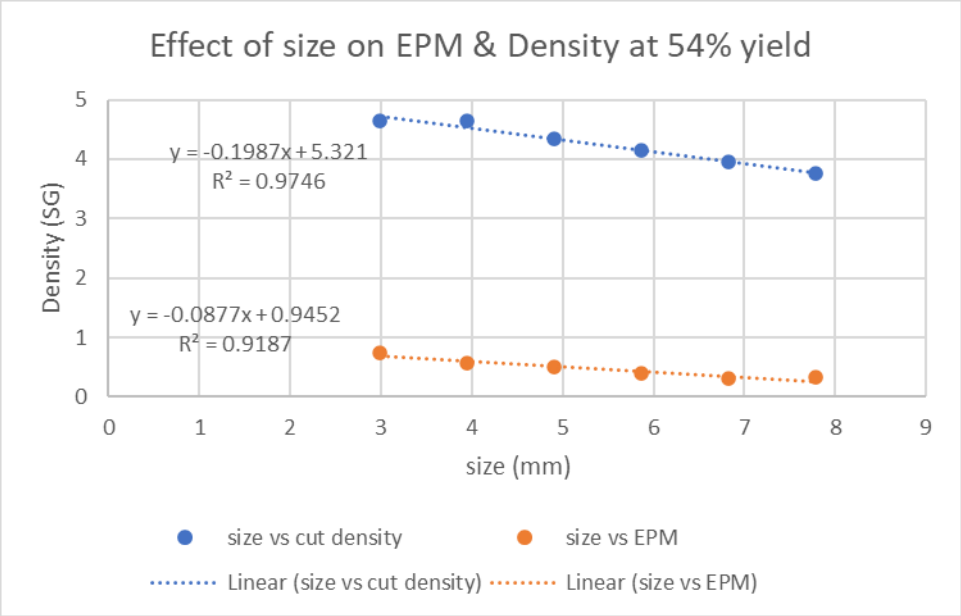


Figure 32: Effect of size on EPM and cut density at 54% yield.

At a yield of 54%, the cut density decreases as the size increases, while EPM slightly decreases as particle size increases.

Table 9: Table showing the influence of size on EPM and cut density at 69% yield.

69% Yield		
Size class	rho50	EPM
7.78	3.222013	0.424224
6.82	3.778253	0.207198
5.86	3.859558	0.367789
4.9	3.993748	0.438384
3.94	4.215173	0.539177
2.99	4.12021	1.015411

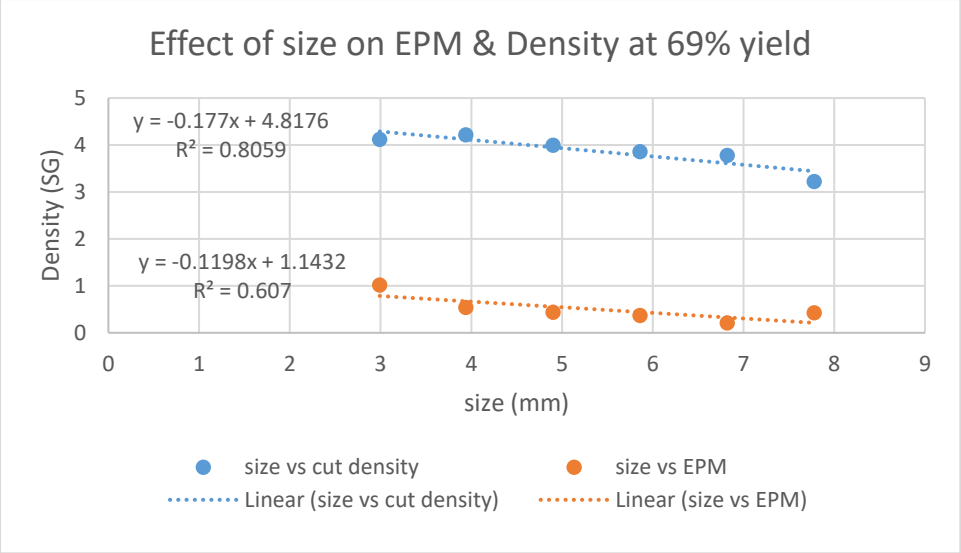


Figure 33:Effect of size on EPM and cut density at 69% yield.

At a yield of 69%, the cut density decreases from 4.1 to 3.2 SG as the size increases, while EPM decreases as size increase with an abnormal increase for large particles, i.e., in the size class of 7.78 mm.

Table 10: Table showing the influence of size on EPM and cut density at 83% yield.

83% Yield		
Size class	rho50	EPM
6.82	3.619952	0.155832
5.86	3.482591	0.370007
4.9	3.611483	0.381899
3.94	3.74719	0.518262
2.99	3.794032	0.497477

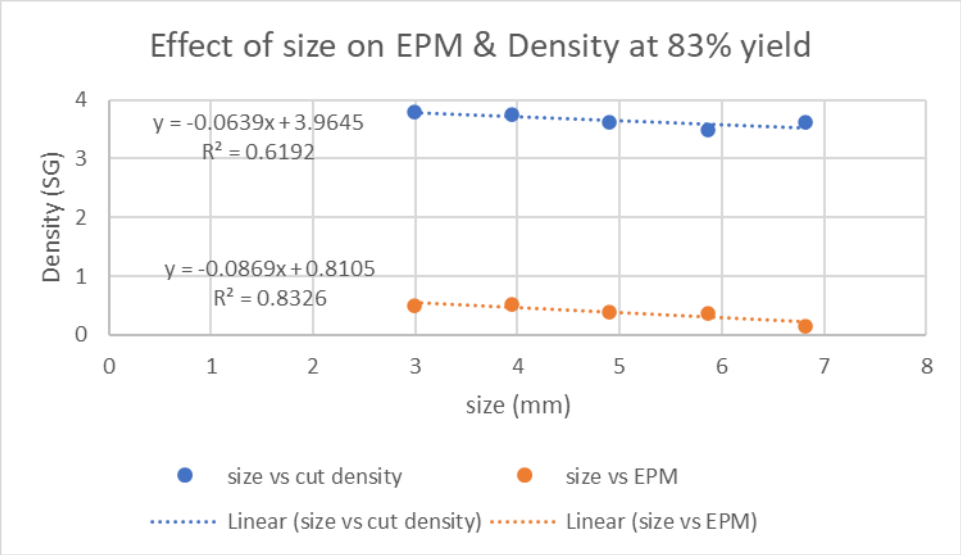


Figure 34: Effect of size on EPM and cut density at 83% yield.

At a yield of 83%, both the cut density and EPM slightly decrease as particle size increases.

Appendix B: Evaluation of particle size effect on EPM and cut density as cut height increases.

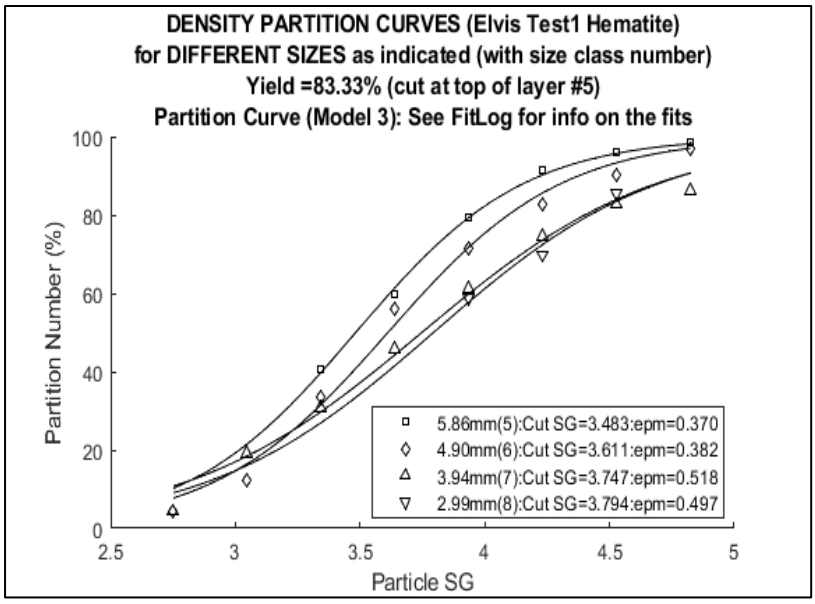


Figure 35: Partition Curves for different sizes.

The density partition curve gets sharper, i.e., EPM decreases, as the yield increases, showing that cutting the bed at a higher layer gives a good representation of the separation process.

Appendix C: tables showing data used to plot effect of particle size on density partition number of particles with SG=4.231

Table 11: Fit LOG data.

	Fit LOG data						
Yield	rho50	epm	Ic	lambda	Variance	Std Dev	Model #
16.40%	4.98480619	0.413578	0.082968	13.2461	0.000125	0.011181	3
39.50%	4.47992511	0.433631	0.096794	11.35399	0.000713	0.02671	3
54.09%	4.20911305	0.425001	0.100972	10.88426	0.000774	0.027813	3
69.24%	3.90743186	0.400404	0.102472	10.72485	0.000846	0.029081	3
83.33%	3.5542077	0.373743	0.105155	10.45122	0.001063	0.032601	3

Data analysis was conducted using jig performance indicators, which accounted for EPM, cut density, and imperfections.

Table 12: Partition data for SG class 3.

	Layer = 1		Layer = 2		Layer = 3		Layer = 4		Layer = 5	
	Yield= 16.4%		Yield= 39.5%		Yield= 54.09%		Yield= 69.24%		Yield= 83.33%	
	SG= 4.231		SG= 4.231		SG= 4.231		SG= 4.231		SG= 4.231	
	SG class No=3		SG class No=3		SG class No=3		SG class No=3		SG class No=3	
Size class number ↓	Partition No for SG class =3	Size (mm)	Partition No for SG class	Size (mm)	Partition No for SG class =3	Size (mm)	Partition No for SG class =3	Size (mm)	Partition No for SG class =3	Size (mm)
3	28.92474035	7.78	66.01834319	7.78	83.81944895	7.78	93.48835773	7.78	96.6761244	7.78
4	21.84409718	6.82	54.06000337	6.82	71.35258803	6.82	86.93878114	6.82	95.42150051	6.82
5	13.76123998	5.86	39.1847571	5.86	57.6807757	5.86	76.8819772	5.86	91.26690501	5.86
6	7.529928816	4.9	28.17138944	4.9	44.27707018	4.9	62.17898502	4.9	82.74658009	4.9
7	5.578521419	3.94	19.39482791	3.94	32.78723813	3.94	52.00445799	3.94	74.46727231	3.94
8	3.072528457	2.99	14.47762291	2.99	30.0116322	2.99	52.17396766	2.99	69.90080019	2.99

Table 13: Parameters for linear fits to plot.

Parameters for linear fits to plot			
P#(%)=m.d(mm)+c			
Yield %	m	c	R^2
16.4	5.4947	-16.119	0.9432
39.5	11.112	-22.915	0.9766
54.09	11.87	-10.56	0.9762
69.24	9.7222	18.29	0.958
83.33	6.1177	52.157	0.958

Appendix D: tables showing output file data for 8x8x4 classes.

Table 14: MATLAB output data for 8x8x4 classes.

Data Name =	Elvis Test1 Hematite												
Source file =	C:\Users\Elvis Dzaringa\Desktop\Updated Program\Test1_All_Layers.xlsx												
	1												
Class Number >>	1	2	3	4	5	6	7	8	9	10	11	12	
SG class Name=	4.825	4.528	4.231	3.935	3.638	3.342	3.045	2.748	#N/A	#N/A	#N/A	#N/A	
Size class Name=	9.69mm	8.73mm	7.78mm	6.82mm	5.86mm	4.90mm	3.94mm	2.99mm	#N/A	#N/A	#N/A	#N/A	
Shape class Name=	0.871	0.713	0.553	0.395	#N/A	#N/A	#N/A	#N/A	#N/A	#N/A	#N/A	#N/A	
Yield/Layer Name	16.40%	39.50%	54.09%	69.24%	83.33%	100.00%	#N/A	#N/A	#N/A	#N/A	#N/A	#N/A	
SG: Class Boundaries (top)	4.973	4.676375	4.37975	4.083125	3.7865	3.489875	3.19325	2.896625	2.6	#N/A	#N/A	#N/A	#N/A
Number particles in class	1128	8808	8018	3140	1187	542	302	373	#N/A	#N/A	#N/A	#N/A	
Average SG (measured)	4.734887	4.508701	4.250058	3.959929	3.655924	3.360555	3.051344	2.74296	#N/A	#N/A	#N/A	#N/A	
%Distribution (by mass)	7.098555	41.21943	32.96021	11.32192	3.877439	1.708692	0.887586	0.926175	#N/A	#N/A	#N/A	#N/A	
Size (mm) Class Boundaries (top)	10.172	9.21375	8.2555	7.29725	6.339	5.38075	4.4225	3.46425	2.506	#N/A	#N/A	#N/A	#N/A
Number particles in class	30	135	513	1573	3359	6566	10990	332	#N/A	#N/A	#N/A	#N/A	
Average size (mm) (measured)	9.612233	8.617867	7.680953	6.740282	5.808072	4.852277	3.940937	3.330542	#N/A	#N/A	#N/A	#N/A	
%Distribution (by mass)	0.813061	2.735876	7.450102	16.14458	22.46873	26.14575	23.72644	0.515455	#N/A	#N/A	#N/A	#N/A	
Shape Factor: Cl Boundaries (top)	0.951	0.792	0.633	0.474	0.315	#N/A	#N/A	#N/A	#N/A	#N/A	#N/A	#N/A	
Number particles in class	2193	11870	8824	611	#N/A	#N/A	#N/A	#N/A	#N/A	#N/A	#N/A	#N/A	
Average Shape Factor (measured)	0.829693	0.704145	0.572287	0.443597	#N/A	#N/A	#N/A	#N/A	#N/A	#N/A	#N/A	#N/A	
%Distribution (by mass)	9.273671	51.34388	37.0904	2.29205	#N/A	#N/A	#N/A	#N/A	#N/A	#N/A	#N/A	#N/A	
BIVARIATE DISTRIBUTIONS													
SIZE class num>>>>>	1	2	3	4	5	6	7	8	9	10	11	12	
SG classes (Class 1)	0.000545	0.002752	0.006852	0.015262	0.015059	0.013892	0.009174	0.000368	#N/A	#N/A	#N/A	#N/A	
2	0.003125	0.009869	0.026976	0.06431	0.092983	0.102434	0.088015	0.002004	#N/A	#N/A	#N/A	#N/A	
3	0.00231	0.00937	0.024951	0.050527	0.070622	0.087714	0.083835	0.001361	#N/A	#N/A	#N/A	#N/A	
4	0.001632	0.002214	0.00903	0.01631	0.026053	0.032955	0.032882	0.000854	#N/A	#N/A	#N/A	#N/A	
5	0.000446	0.001234	0.003076	0.006169	0.008477	0.01315	0.012327	0.00037	#N/A	#N/A	#N/A	#N/A	
6	0	0.000952	0.001105	0.003753	0.00443	0.005717	0.005647	0.000104	#N/A	#N/A	#N/A	#N/A	
7	0	0.000197	0.000723	0.002546	0.003061	0.002663	0.003179	2.52E-05	#N/A	#N/A	#N/A	#N/A	
8	0	0.000785	0.001713	0.001364	0.003126	0.002993	0.004338	8.97E-05	#N/A	#N/A	#N/A	#N/A	
9	#N/A	#N/A	#N/A	#N/A	#N/A	#N/A	#N/A	#N/A	#N/A	#N/A	#N/A	#N/A	
10	#N/A	#N/A	#N/A	#N/A	#N/A	#N/A	#N/A	#N/A	#N/A	#N/A	#N/A	#N/A	
11	#N/A	#N/A	#N/A	#N/A	#N/A	#N/A	#N/A	#N/A	#N/A	#N/A	#N/A	#N/A	
12	#N/A	#N/A	#N/A	#N/A	#N/A	#N/A	#N/A	#N/A	#N/A	#N/A	#N/A	#N/A	
Shape Factor class num>>>>	1	2	3	4	5	6	7	8	9	1	11	12	
Size classes (Class 1)	0	0	0	0	0	0	#N/A	#N/A	#N/A	#N/A	#N/A	#N/A	
2	0	0.000785	0	0	0	0	#N/A	#N/A	#N/A	#N/A	#N/A	#N/A	
3	0	0.000871	0.000842	0	0	0	#N/A	#N/A	#N/A	#N/A	#N/A	#N/A	
4	0	0.00098	0.000383	0	0	0	#N/A	#N/A	#N/A	#N/A	#N/A	#N/A	
5	0.000419	0.00155	0.001004	0.000153	0	0	#N/A	#N/A	#N/A	#N/A	#N/A	#N/A	
6	0.000204	0.001808	0.000928	5.35E-05	0	0	#N/A	#N/A	#N/A	#N/A	#N/A	#N/A	
7	0.000398	0.001981	0.001727	0.000233	0	0	#N/A	#N/A	#N/A	#N/A	#N/A	#N/A	
8	0	3.37E-05	2.55E-05	3.05E-05	0	0	#N/A	#N/A	#N/A	#N/A	#N/A	#N/A	
9	#N/A	#N/A	#N/A	#N/A	#N/A	#N/A	#N/A	#N/A	#N/A	#N/A	#N/A	#N/A	
10	#N/A	#N/A	#N/A	#N/A	#N/A	#N/A	#N/A	#N/A	#N/A	#N/A	#N/A	#N/A	
11	#N/A	#N/A	#N/A	#N/A	#N/A	#N/A	#N/A	#N/A	#N/A	#N/A	#N/A	#N/A	
12	#N/A	#N/A	#N/A	#N/A	#N/A	#N/A	#N/A	#N/A	#N/A	#N/A	#N/A	#N/A	
Partition No for SG class =	1	2	3	4	5	6	7	8	9	10	11	12	
in layer number 1	39.37527	22.64144	13.4181	5.053547	1.277655	0	0	0	#N/A	#N/A	#N/A	#N/A	
2	71.03276	50.42896	36.91275	22.36958	9.595725	1.083325	0	0	#N/A	#N/A	#N/A	#N/A	
3	82.36943	66.41804	53.1318	36.56574	18.7162	6.671041	0.779157	0.151199	#N/A	#N/A	#N/A	#N/A	
4	91.4038	80.8935	70.14914	55.48932	34.36947	16.01258	4.247304	1.612347	#N/A	#N/A	#N/A	#N/A	
5	96.85116	92.10759	85.97909	75.66975	55.77975	40.40183	14.89819	3.959371	#N/A	#N/A	#N/A	#N/A	
6	100	100	100	100	100	100	100	100	#N/A	#N/A	#N/A	#N/A	
7	#N/A	#N/A	#N/A	#N/A	#N/A	#N/A	#N/A	#N/A	#N/A	#N/A	#N/A	#N/A	
8	#N/A	#N/A	#N/A	#N/A	#N/A	#N/A	#N/A	#N/A	#N/A	#N/A	#N/A	#N/A	
9	#N/A	#N/A	#N/A	#N/A	#N/A	#N/A	#N/A	#N/A	#N/A	#N/A	#N/A	#N/A	
10	#N/A	#N/A	#N/A	#N/A	#N/A	#N/A	#N/A	#N/A	#N/A	#N/A	#N/A	#N/A	
Yield	16.40%	39.50%	54.09%	69.24%	83.33%	100.00%	#N/A	#N/A	#N/A	#N/A	#N/A	#N/A	